Molecular Pharmacology Fast Forward. Published on December 16, 2013 as doi: 10.1124/mol.113.090530

MOL #90530

Recovery of current through mutated TASK3 potassium channels underlying Birk Barel syndrome

Emma L Veale, Mustafa Hassan, Yvonne Walsh, Ehab Al-Moubarak, Alistair Mathie

Medway School of Pharmacy, University of Kent and University of Greenwich, Central Avenue, Chatham Maritime, Kent, UK. ME4 4TB.

Molecular Pharmacology Fast Forward. Published on December 16, 2013 as DOI: 10.1124/mol.113.090530
This article has not been copyedited and formatted. The final version may differ from this version.

Running title: Recovery of current in mutated TASK3 channels

To whom correspondence should be addressed: Alistair Mathie, Medway School of Pharmacy, University of Kent, Central Avenue, Chatham Maritime, Kent, ME4 4TB, UK. Phone: 01634 202955 Fax: 01634 883927 Email: a.a.mathie@kent.ac.uk

Text Pages: 22

Tables: 0

Figures: 7

References: 50

Abstract: 229 words

Introduction: 493 words

Discussion: 1242 words

Non Standard Abbreviations

FFA	flufenamic acid, 2-{[3-(Trifluoromethyl)phenyl]amino}benzoic acid
GFP	green fluorescent protein
K2P	two pore domain potassium
TASK	TWIK-related acid-sensitive K
TM	transmembrane domain
TRAAK	TWIK-related arachidonic acid activated K
WT	wild type

Molecular Pharmacology Fast Forward. Published on December 16, 2013 as DOI: 10.1124/mol.113.090530
This article has not been copyedited and formatted. The final version may differ from this version.

Abstract

TASK3 potassium channels are members of the two pore domain potassium channel family. They are responsible for background leak potassium currents found in many cell types. TASK3 channels are genetically imprinted and a mutation in TASK3 (G236R) is responsible for a maternally transmitted developmental disorder, Birk Barel mental retardation dysmorphism syndrome. This syndrome may arise from a neuronal migration defect during development caused by dysfunctional TASK3 channels. Through the use of whole-cell electrophysiological recordings, we have found that although G236R mutated TASK3 channels give rise to a functional current, this current is significantly smaller in an outward direction when compared to wild type (WT) TASK3 channels. In contrast to WT TASK3 channels, the current is inwardly-rectifying. Furthermore, the current through mutated channels is differentially sensitive to a number of regulators such as extracellular acidification, extracellular zinc and activation of Gαq-coupled muscarinic (M3) receptors compared with WT TASK3 channels. The reduced outward current through mutated TASK3_G236R channels can be overcome, at least in part, by both a gain of function additional mutation of TASK3 channels (A237T) or by application of the non-steroidal anti-inflammatory drug, flufenamic acid. Flufenamic acid produces a significantly greater enhancement of current through mutated channels than through WT TASK3 channels. We propose that pharmacological enhancement of mutated TASK3 channel current during development may, therefore, provide a potentially useful therapeutic strategy in the treatment of Birk Barel syndrome.

Molecular Pharmacology Fast Forward. Published on December 16, 2013 as DOI: 10.1124/mol.113.090530
This article has not been copyedited and formatted. The final version may differ from this version.

Introduction

TASK3 (TWIK-related acid-sensitive K channel 3, KCNK9, $K_{2P}9.1$) channels are members of the two pore domain potassium (K2P) channel family (Goldstein *et al,* 2005; Enyedi and Czirjak, 2010). The TASK channels TASK1 and TASK3, as their name suggests, are highly sensitive to changes in extracellular pH (Duprat *et al,* 1997; Kim *et al,* 2000; Rajan *et al,* 2000; González *et al,* 2013). Extracellular acidification reduces TASK3 channel current. Other agents such as extracellular application of zinc and ruthenium red, the synthetic cannabinoid, methanandamide and activation of Gαq-coupled receptors, including M_3 muscarinic acetylcholine receptors, inhibit TASK3 channels (Czirjak and Enyedi, 2003; Clarke et al, 2004; Veale *et al,* 2007a,b; Clarke *et al,* 2008) and consequently the native currents that they encode (e.g. Aller *et al,* 2007). In most cases, these agents work by altering channel gating.

TASK3 channels are widely distributed throughout the body, with notable expression in the central nervous system (Talley *et al,* 2001). They are responsible for native leak K currents found in many cell types including neurons such as cerebellar granule neurons (CGNs), where they are a major component of the background leak K current IK_{SO} (Aller *et al,* 2007; Watkins and Mathie, 1996; Millar *et al,* 2000). TASK3 channels also play an important role in the migration of cortical pyramidal neurons during development (Bando *et al,* 2012) and TASK3 knock-out mice show abnormalities in certain cognitive functions (Linden et al, 2007). TASK3 channels are proposed to play a role in various pathological conditions such as epilepsy (Kananura *et al,* 2002), cancer (Mu *et al,* 2003; Pei *et al,* 2003), ischaemia (Ehling *et al,* 2010), idiopathic hyperaldosteronism, particularly in neonates (Davies *et al,* 2008; Bandulik et al 2013) and low renin essential hypertension (Guagliardo *et al,* 2012; Penton *et al,* 2012).

TASK3 channels are the only K2P channels known to be genetically imprinted, in that they are expressed only from the maternal allele (Luedi *et al,* 2007). Indeed a mutation in TASK3 (G236R) is responsible for a maternally transmitted developmental disorder, Birk Barel mental retardation dysmorphism syndrome (Barel *et al,* 2008). It has been proposed that the migration defect caused by dysfunctional TASK3 channels in cortical pyramidal neurons may contribute to the resulting developmental disorders (Bando *et al,* 2012).

In this study we have considered the functional properties of G236R mutated TASK3 channels in more detail. We show that expression of TASK3_G236R channels does, in fact,

Molecular Pharmacology Fast Forward. Published on December 16, 2013 as DOI: 10.1124/mol.113.090530
This article has not been copyedited and formatted. The final version may differ from this version.

give rise to a functional current, albeit a much smaller current in an outward direction compared to WT TASK3. In contrast to WT TASK3 channels, the current is inwardly rectifying and this current is differentially sensitive to a number of regulators such as extracellular acidification and activation of G protein coupled receptors. Importantly, the reduced current through mutated TASK3_G236R channels can be overcome, at least in part, by both a gain of function additional mutation of TASK3 channels (A237T, Ashmole *et al,* 2009) or by application of the non-steroidal anti-inflammatory drug, flufenamic acid (FFA).

Materials and Methods

Cell culture

tsA201 cells (ECACC, Sigma-Aldrich, Gillingham, Dorset, UK), modified human embryonic kidney 293 cells, were grown in a monolayer tissue culture flask maintained in a growth medium which was composed of 88% minimum essential media with Earle's salts and 2mM L-glutamine, 10% of heat-inactivated fetal bovine serum, 1% penicillin (10,000 units ml^{-1}) and streptomycin (10 mg ml^{-1}), and 1% non-essential amino acids. The cells were placed in an incubator at 37^{o}C with a humidified atmosphere of 95% oxygen and 5% carbon dioxide. After 2 or 3 days, when the cells were 70 to 90% confluent, they were split and resuspended in a 4 well plate containing 13 mm diameter cover slips (poly-D-lysine coated) in 0.5 ml of media, ready to be transfected the next day.

Transfection

For the electrophysiological experiments, the pcDNA3.1 vector was cloned with the gene of interest (hTASK3 or mTASK3 wild-type and mutated and hM3 muscarinic receptors). This and a similar vector containing GFP were incorporated into the tsA201 cells (0.5 µg per well for hTASK3, hM3 muscarinic receptors and GFP plasmids, 0.125 µg per well for mTASK3 plasmids) using the calcium phosphate method. The cells were incubated for 6 - 12 hours at 37^{o}C in 95% oxygen and 5% carbon dioxide. Cells were then washed using a phosphate buffered saline solution (PBS), and new media was added to each well. The cells were used for experiments after 24 hours.

Mutations

Point mutations were introduced by site-directed mutagenesis into the TASK3 channel clones using the Quikchange kit (Stratagene, Amsterdam, The Netherlands). A pair of short (25 - 35 bases) complementary oligonucleotide primers, incorporating the intended mutation, were synthesized (Eurofins MWG Operon, Ebersberg, Germany). Mutant DNA constructs

Molecular Pharmacology Fast Forward. Published on December 16, 2013 as DOI: 10.1124/mol.113.090530
This article has not been copyedited and formatted. The final version may differ from this version.

were sequenced (Eurofins MWG Operon) to confirm the introduction of the correct mutated bases.

Whole cell patch clamp electrophysiology

Currents were recorded using the whole cell patch clamp in a voltage clamp configuration in tsA201 cells transiently transfected with the channel of interest. The cover slip with the cells was placed in a recording chamber filled with an external medium composed of 145 mM, NaCl, 2.5 mM KCl, 3 mM $MgCl_2$, 1 mM $CaCl_2$ and 10 mM HEPES (pH to 7.4, using NaOH). The internal medium used in the glass pipette comprised 150 mM KCl, 3 mM $MgCl_2$, 5 mM EGTA and 10 mM HEPES (pH to 7.4, using KOH). Modulatory compounds were applied by bath perfusion at a rate of 4-5 ml min^{-1}. Complete exchange of bath solution occurred within 100-120s.

All the data presented have been collected at room temperature (19-22^{o}C). The transfected cells were detected using a fluorescent microscope with UV light. Cells were voltage-clamped using an Axopatch 1D or Axopatch 200B amplifier (Molecular Devices, Sunnyvale, CA, USA) and low pass filtered at 5 kHz before sampling (2-10 kHz) and online capture.
In order to study the potassium leak current, a ”step-ramp” voltage protocol was used. For the step component of the protocol, cells were hyperpolarised from a holding voltage of -60 mV to -80 mV for 100ms then stepped to -40 mV for 500 ms. For the ramp, cells were then stepped to -120 mV for 100 ms, followed by a 500 ms voltage ramp to +20 mV and a step back to -80 mV for another 100 ms, before being returned to the holding voltage of -60 mV. This protocol was composed of sweeps lasted 1.5 seconds (including sampling at the holding voltage) and was repeated once every 5 seconds. An example of the typical current response seen for WT TASK3 channels to this protocol is illustrated in Fig. 1*D*.
For analysis of outward current, we measured the current difference between the - 80 mV and - 40 mV steps. The current-voltage graphs were obtained from the ramp change in voltage between -120 mV and + 20 mV. The currents obtained with the imposed voltage protocol were recorded and analysed using pCLAMP 10.2 software and Microsoft Excel. For each cell, the current amplitude (pA) was normalised to the cell capacitance (pF).

Data analysis

Data were expressed as mean ± standard error of the mean (SEM) and ‘n’ represents the number of cells used for the experiment. The statistical analyses used either the Student t-test or a one way ANOVA with the post-hoc Dunnett’s or Tukey multiple comparisons tests, using GraphPad Prism 6.02. For the t-test, the differences between means were considered

Molecular Pharmacology Fast Forward. Published on December 16, 2013 as DOI: 10.1124/mol.113.090530
This article has not been copyedited and formatted. The final version may differ from this version.

as significant for $p < 0.05$ (*), $p < 0.01$ (**) and $p < 0.001$ (***). For the Dunnett's and Tukey's tests, data were considered significantly different at the < 0.05 level (*); confidence interval > 95% for the difference between the two compared means.

Chemicals

All fine chemicals were purchased from Sigma-Aldrich, Gillingham, Dorset, UK. Flufenamic acid (FFA) stock (10 mM) was made up in ethanol and diluted fresh in external solution before use (pH adjusted to 7.4).

Homology Modelling

The homology models of hTASK3 (UniProtKB/Swiss-Prot ID: Q9NPC2) and mTASK3 (UniProtKB/Swiss-Prot ID: Q3LS21) were created using Modeller 9v8 (Sali and Blundell, 1993). The human TRAAK structure (PDB ID: 3UM7) was used as a template for TASK3 modelling. ClustalW (Higgins *et al,* 1996) was used to align the TRAAK and TASK3 sequences.

Results

Characterisation of current through G236R mutated TASK3 channels. Following conversion of the glycine (G) residue at position 236 of the human (h) TASK3 channel into an arginine (R) residue, currents through wild type (WT) and mutated channels were recorded in transiently transfected tsA201 cells using whole-cell patch-clamp recordings. Outward current density was significantly reduced by 85% from 66 ± 3 pA/pF (n = 56) for WT TASK3 to 10 ± 1 pA/pF (n = 17) for TASK3_G236R mutated channels ($p < 0.001$) when assessed as the difference current between that measured at -40 mV and that at -80 mV (see materials and methods, Fig. 1*A*). Nevertheless, in these experiments, there was still measurable current seen for this G236R mutation, in contrast to the lack of current in untransfected cells (Supplemental Figure 1). This is also in contrast to results obtained for the same mutation expressed in oocytes by Barel *et al,* (2008), who described the TASK3_G236R mutant as non-functional. Unlike WT TASK3 channel current which is outwardly rectifying (Fig. 1*D*), there was substantial inward rectification of current through the TASK3_G236R channel (Fig. 1*G*). Indeed, when inward current density was measured at -120 mV, there was no significant difference ($p > 0.05$) between WT TASK3 and TASK3_G236R (28 ± 3 pA/pF, n = 46, and 20 ± 2 pA/pF, n = 17, respectively, Fig. 1*B*). An identical effect was seen for mouse (m) TASK3 channels. Outward current (difference current between -40 and -80 mV) through mutated mTASK3_G236R channels was reduced by 83% compared to WT mTASK3 channels and the current through the mutated channels was also inwardly-rectifying (Supplemental Figure 2).

Molecular Pharmacology Fast Forward. Published on December 16, 2013 as DOI: 10.1124/mol.113.090530
This article has not been copyedited and formatted. The final version may differ from this version.

With a physiological extracellular solution containing 2.5 mM $[K^+]_o$, the hTASK3_G236R channel had an average reversal potential of -72 ± 1 mV (n = 17). This suggests a slight reduction in K selectivity, with a Na permeability (relative to K) calculated from the Goldman-Hodgkin-Katz equation of 0.04 compared to <0.02 for WT TASK3 (see also Fig. 1*C*). When the external K was increased to 25 mM or 147.5 mM $[K^+]_o$ and $[Na^+]_o$ correspondingly reduced, TASK3_G236R channels conducted relatively large inward currents with reversal potentials of -36 ± 2 mV (n = 5), (compared to -40 ± 1 mV, n = 15, for WT TASK3) in 25 mM $[K^+]_o$ and +4 ± 3 mV (n = 5) in 147.5 mM $[K^+]_o$ (compared to -12 ± 1 mV, n = 4, for WT TASK3) (Fig. 1*C, E, H*). Interestingly, the slope of the current in 25 mM or 147.5 mM $[K^+]_o$ still showed strong inward rectification (Fig. 1*H*). Similarly, when the $[K^+]_o$ was replaced by 25 mM or 147.5 mM $[Rb^+]_o$, TASK3_G236R channels again conducted relatively large inward currents with reversal potentials of -31 ± 1 mV (n = 3) (compared to -48 ± 1 mV, n = 12, for WT TASK3) in 25 mM $[Rb^+]_o$ and +4 ± 1 mV (n = 3) in 147.5 $[Rb^+]_o$ (compared to -5 ± 3 mV, *n* = 3, for WT TASK3) (Fig. 1*F,I*). So, like WT TASK3 channels, TASK3_G236R channels are highly permeable to Rb, with a permeability relative to K of 1.00 when compared at 147.5 mM of each ion, externally. Again, the slope of the current in high $[Rb^+]_o$ showed inward rectification (Fig 1*I*). Reduction of internal magnesium from 3 mM to 1 mM did not alter the degree of inward rectification of the current.

TASK3 channel structure. We have created an updated model of hTASK3 and mTASK3 channels based on the recent crystal structure of the related K2P channel TRAAK (Brohawn *et al,* 2012) (Fig. 2 and Supplemental Figure 3). There are substantial differences in the amino acid sequences of hTASK3 and mTASK3 channels, however, whilst they share only 44% sequence similarity in the C terminus region, for which the structure is unknown, they have 98% similarity in the remainder of the channel (Veale *et al,* 2007b). Therefore, the structures of hTASK3 and mTASK3 in the transmembrane regions and pore domains, based on the solved structure for TRAAK, are very similar to each other. We have altered the structures to indicate the position of G236 (mutated to R) in the 4th transmembrane domain (TM4) of the channel and also the adjacent amino acid A237 (mutated to T, see below) (Fig. 2). Charged amino acids are highlighted in the structures (blue for positively charged amino acids and red for negatively charged amino acids). It can be seen that both hTASK3 and mTASK3 models show that introduction of an R at position 236, in addition to influencing the

Molecular Pharmacology Fast Forward. Published on December 16, 2013 as DOI: 10.1124/mol.113.090530
This article has not been copyedited and formatted. The final version may differ from this version.

structure and mobility of TM4, will introduce a positively charged amino acid into the pore cavity of the channel, a region lacking endogenously charged amino acids.

The gain of function mutation A237T of TASK3 channels. It is known from previous work (Ashmole *et al,* 2009, De la Cruz *et al,* 2003) that mutation of the alanine immediately adjacent to G236 to a threonine residue (A237T) results in a gain of function mutation with much larger (> 10 fold) whole cell current compared to WT TASK3 channels. It has been suggested that this mutation alters the gating of the TASK3 channel, so that the channel spends more time in its open conformation (Ashmole *et al,* 2009).

It was of interest to determine whether either the substantial reduction in channel current, or the inward rectification seen for the G236R mutated channels, or both, could be reversed by this gain of function mutation or whether the effects of the G236R mutation were insurmountable. Furthermore, the TM4 region of K2P channels has been suggested to be crucial in transducing gating signals from the cytoplasmic side of the channel to the selectivity filter gate (Bagriantsev *et al,* 2011, 2012, Piechotta *et al,* 2011), so we sought to determine whether mutations of amino acids in this region interfered with gating and regulation of TASK3 channels.

Combining the G236R mutation with A237T rescued current through this double mutated channel compared with G236R alone (Fig. 3*A*). The double mutation significantly (< 0.05, ANOVA with Tukey test, Fig. 3A) increased the outward current density measured as the difference current between that at -40 mV and that at -80 mV from 10 ± 1 pA/pF (n = 17) to 20 ± 3 pA/pF (n = 12) at 2.5 mM $[K^+]_o$, with a reversal potential for currents through the double mutant channel of -80 ± 2 mV (n = 12). However, despite an increase in current, the addition of A237T did not rescue outward current to normal WT levels at these voltages (Fig. 3A). Furthermore, addition of the A237T mutation was not able to overcome the inward rectification seen with the G236R mutation (Fig. 3*B*). However inward current density measured at -120 mV was 31 ± 5 pA/pF (n = 12), which was not significantly different from WT TASK3 current density at this holding potential (see above).

In 25 mM $[K^+]_o$, inward current density at -80 mV was 36 ± 5 pA/pF (n = 5) for TASK3_G236R alone but this increased to 76 ± 7 pA/pF (n = 4) for the TASK3_G236R_A237T channels, the latter not significantly different from that seen for WT TASK3 (85 ± 7 pA/pF, n = 19) (Fig. 3*C*). Similar results were obtained when the extracellular solution contained 25 mM $[Rb^+]_o$. Current at -80 mV, in 25 mM $[Rb^+]_o$, was 11 ± 1 pA/pF (n =

Molecular Pharmacology Fast Forward. Published on December 16, 2013 as DOI: 10.1124/mol.113.090530
This article has not been copyedited and formatted. The final version may differ from this version.

3) for TASK3_G236R alone but this increased to 19 ± 4 pA/pF (n = 6) for the TASK3_G236R_A237T channels, the latter again not significantly different from that seen for WT TASK3 (17 ± 4 pA/pF, n = 12) (Fig. 3*E*). For both 25 mM $[K^+]_o$ and $[Rb^+]_o$, the currents through the TASK3_G236R_A237T channels continued to display strong inward rectification, in contrast to WT TASK3 currents (Fig. 3*D, F*). Mutated TASK3_A237T channels were outwardly rectifying like WT TASK3 channels.

Sensitivity of G236R mutated TASK3 channels to extracellular acidification and zinc. Two characteristic inhibitors of TASK3 channels are extracellular acidification (Aller *et al,* 2005) and extracellular application of zinc (Clarke *et al,* 2004, 2008). Both of these regulators were still effective inhibitors of TASK3_G236R, although in both cases there was a small but significant reduction in their effectiveness. A change in pH_O from 7.4 to 6.4 decreased TASK3_G236R current by 30 ± 7% (n = 3). This was significantly different from that seen with WT TASK3 (61 ± 2%, n = 21, P < 0.001) (Fig. 4*A, B*). Increasing external pH from 7.4 to 8.4 did not enhance current through either WT or mutated TASK3 channels. Zinc at 100 µM is a very potent blocker of WT TASK3 current (87 ± 1%, n = 23). It was also a potent blocker of the TASK3_G236R channels (74 ± 1%, n=3). However, this was significantly smaller than inhibition seen for WT TASK3 (P<0.003) (Fig. 4*C, D*).

TASK3_A237T and TASK3_G236R_A237T mutated channels were still inhibited by zinc and external acidification, but as for TASK3_G236R channels, the effect of external acidification was less than that seen for WT channels. The TASK3_A237T mutant alone saw a reduced effect of pH 6.4 with a current inhibition of 41 ± 2% (n = 9) which was significantly less than that seen for WT TASK3 (61 ± 2%, n = 21, p < 0.001). Similarly, a change in pH_O from 7.4 to 6.4 inhibited TASK3_G236R_A237T current by just 31 ± 3 % (n = 6). Zinc (100 µM) inhibited the TASK3_A237T mutation alone by 87 ± 5 % (n = 3), not significantly different to that seen for WT TASK3 current and the TASK3_G236R_A237T channels by 78 ± 2 % (n = 4).

Regulation of TASK3 channels by M3 muscarinic receptor activation. TASK3 channels are regulated by activation of Gαq-coupled receptors such as M3 muscarinic receptors (Veale *et al,* 2007b). When TASK3 channels were co-expressed with muscarinic M3 receptors, application of the muscarinic agonist, muscarine (0.1 µM) resulted in an inhibition of the TASK3 current of 75 ± 2% (n = 34) which was reversed by wash (Fig. 5*A*). However, unlike WT TASK3, no inhibition of the current through TASK3_G236R channels was observed at 0.1 µM muscarine (5 ± 7% *enhancement,* n = 3, P < 0.001) (Fig. 5*C*). Higher

Molecular Pharmacology Fast Forward. Published on December 16, 2013 as DOI: 10.1124/mol.113.090530
This article has not been copyedited and formatted. The final version may differ from this version.

concentrations of muscarine were applied to determine whether the concentration response curve for muscarine had shifted for the G236R mutant. However neither 1 nor 10 µM muscarine had any inhibitory effect on TASK3_G236R (1 ± 2 %, enhancement, n = 3; 8 ± 5 %, n = 4, enhancement, for 1 and 10 µM respectively) (Fig. 5*A-D*). It is of interest that the effect of muscarine was also reduced in the gain of function TASK3_A237T mutant channel, although not to the same degree. The TASK3_A237T channel was inhibited by just 13 ± 3% (n = 6) by 0.1 µM muscarine. Larger inhibitory effects could be seen at higher concentrations of muscarine (31 ± 4%, n = 5, for 1 µM and 35 ± 7%, n = 4 for 10 µM), although these were still significantly smaller than that seen for WT TASK3 (86 ± 4 %, n = 6, and 91 ± 1%, n = 3, for 1 and 10 µM respectively) (Fig. 5*E, F*).

Flufenamic-acid induced enhancement of TASK3 current. Other than certain inhalational general anesthetic agents, there are relatively few compounds available that enhance TASK3 currents. One is the fenamate, flufenamic acid (FFA), which has been shown previously to enhance current through other K2P channels (Takahira *et al,* 2005) and which produces a small but significant enhancement of current by 24 ± 6% (n = 8) at a concentration of 100 µM (Fig. 6*A-D*). Surprisingly, application of 100 µM FFA produced a robust and significant enhancement of 154 ± 11% (n = 7) of TASK3_G236R channels, significantly greater that that seen for WT TASK3 channels ($p < 0.001$). This resulted in an increase in outward current density from 10 ± 1 pA/pF (*n* = 17) to 32 ± 6 pA/pF (*n* = 7) and a shift in the reversal potential from -72 ± 1 mV (*n* = 17) to -87 ± 2 mV (*n* = 7) in the presence of FFA (Fig. 6*E-G*). Nevertheless, even this FFA-enhanced current through TASK3_G236R channels showed inward rectification. The effect of FFA on the double mutant (TASK3_G236R_A237T channels) was much reduced compared to the TASK3_G236R mutant, but was similar to that seen for WT TASK3 with an enhancement of 36 ± 3 % (n = 4) (Fig. 6*H-J*). FFA had no effect on the TASK3_A237T mutant channel with 2 ± 1 % (n = 3) enhancement seen.

Characterisation of current through G236F mutated TASK3 channels. The G236 amino acid was altered to a bulky but uncharged amino acid, phenylalanine (F). This TASK3_G236F mutation resulted in a reduced outward current density to 14 ± 1 pA/pF (*n*=21) in 2.5 mM $[K^+]_o$ when measured as the difference current between that at -40 mV and -80 mV (Fig. 7*A*). However, unlike the TASK3_G236R mutation, inward current density measured at -120 mV was also reduced by the TASK3_G236F mutation (to 9 ± 1 pA/pF, *n*=21, $p < 0.005$) (Fig. 7*B*). The TASK3_G236F mutation also did not display the inward

Molecular Pharmacology Fast Forward. Published on December 16, 2013 as DOI: 10.1124/mol.113.090530
This article has not been copyedited and formatted. The final version may differ from this version.

rectification that was seen with the TASK3_G236R mutant – the current resembling a reduced amplitude wild-type TASK3 current (Fig. 7*C*).

The TASK3_G236F mutant channel was not enhanced beyond that seen for WT TASK3 by FFA. Application of 100 µM FFA gave an average enhancement of 17 ± 3 % (*n* = 5) p > 0.05 (Fig. 7 *D-F*). However, the TASK3_G236F mutant channel was differentially regulated by muscarine compared to WT TASK3 with 1 µM muscarine inhibiting current by just 19 ± 5 % (n = 5) (Fig. 7 *G-I*). The TASK3_G236F mutant channel showed the same sensitivity as WT TASK3 channels to block following extracellular acidification and extracellular zinc (Fig. 7*J-O*). A change in pH_O from 7.4 to 6.4 decreased TASK3_G236F current by 70 ± 1 % (n = 4), whilst zinc (100 µM) inhibited the TASK3_G236F current by 92 ± 1 % (n = 5). Thus it appears that the inward rectification and regulation by FFA, extracellular acidification and zinc of TASK3 channels mutated at position G236 depends on the nature of the substituted residue, but that the outward current density and Gαq mediated regulation is altered by both charged and uncharged bulky amino acid substitutions.

Discussion

A point mutation of G236 to an R in TASK3 is found in patients suffering from Birk Barel mental retardation dysmorphism syndrome (Barel *et al,* 2008). In this study, we show that TASK3_G236R does, in fact, give rise to a functional current, albeit with much smaller currents in an outward direction. In contrast to WT TASK3 channels, the current is inwardly rectifying.

Inward rectification of potassium channels is most clearly associated with the inward rectifier (K_{IR}) family of K channels. For these channels, this inward rectification occurs because currents at voltages positive to E_K are blocked by intracellular Mg^{2+} or polyamines such as spermine. The positively charged internal Mg^{2+} ions and/or internal polyamines are attracted to primarily negatively charged residues, localized in both the transmembrane domains lining the channel pore and the cytoplasmic regions of these channels and physically block permeation (Hibino *et al,* 2010). The K2P channels, TWIK1 and TWIK2 display weak inward rectification at positive voltages. For TWIK2, it is proposed that this rectification is due to an intrinsic time-dependent inactivation at positive voltages (Patel *et al,* 2000). TASK2 channels have also been shown to possess mild inward rectification, caused by block by internal Na ions acting at the selectivity filter (Morton *et al,* 2005).

Molecular Pharmacology Fast Forward. Published on December 16, 2013 as DOI: 10.1124/mol.113.090530
This article has not been copyedited and formatted. The final version may differ from this version.

In the case of TASK3_G236R channels, it is the presence of an introduced positively charged amino acid in the TM4 transmembrane domain at the cytoplasmic end of the inner vestibule that results in inward rectification not seen for WT TASK3 channels. Intrinsic inward rectification has been described previously for WT small conductance, calcium-activated K (SK) channels (Li and Aldrich, 2011).

In TASK3, mutation G236F at this position instead of R, reduced current density but did not induce inward rectification. The non-selective cation channel, NaK (Alam and Jiang, 2009) has an F residue at the equivalent position to G236 in TASK3 (F92). This residue, located within the cavity of the channel pore, was suggested to form a constriction point within the open pore, restricting ion flux through the NaK channel. Mutating this residue to A (F92A) increased ion conduction rates as measured by ^{86}Rb flux assays (Alam and Jiang, 2009).

The *C elegans* protein, SUP-9, is a K2P channel with sequence similarity to hTASK1 and hTASK3 channels. A mutant threonine (A236T) in the TM4 of SUP-9 results in a channel that is constitutively open (De la Cruz *et al,* 2003). Introducing a threonine residue at the equivalent position in hTASK3 (replacing alanine, A237T) can also increase the open probability for TASK3 channels by several fold (Ashmole *et al,* 2009). It was suggested that this introduced threonine residue in TM4 stabilises the open state of the channel through altered side-chain interactions between residues, possibly with N133 in TM2. TASK3 channel activity is moderately sensitive to membrane potential and this voltage dependence was altered in the A237T mutated TASK3 channel (Ashmole *et al,* 2009).

In this study, we have found that this gain of function A237T mutation reduces the sensitivity of TASK3 channels to regulation by muscarinic receptor activation. It also has a small effect on sensitivity to extracellular acidification but no detectable effect on zinc mediated inhibition of the channel. Taken together with the observation that this mutation alters the sensitivity of the channel to changes in membrane voltage (Ashmole *et al,* 2009), it is clear that this mutation, like mutation of the adjacent G236 residue, influences channel gating.

Gating and regulation of TASK3 channels. Like other K channels, K2P channels were proposed to have two primary conserved gating mechanisms (Mathie *et al,* 2010). These are an inactivation (or C-type) gate at the selectivity filter close to the extracellular side of the channel (Cohen *et al,* 2009) and an activation gate at the bundle crossing region of the channel (Ben-Abu *et al,* 2009; Cohen *et al,* 2009). For TASK3 channels, there is good evidence that regulators such as extracellular acidification (Kim *et al,* 2000; Rajan *et al,* 2000; Ma *et al,* 2012; González *et al,* 2013) and extracellular zinc (Clarke *et al,* 2004, 2008;

Molecular Pharmacology Fast Forward. Published on December 16, 2013 as DOI: 10.1124/mol.113.090530
This article has not been copyedited and formatted. The final version may differ from this version.

González *et al,* 2013) act at the selectivity filter to gate the channel. It is less clear, however, whether intracellular regulators, such as those arising following activation of Gαq, interact with the bundle crossing gate or the selectivity filter gate or even whether the bundle crossing region acts as a true gate of K2P channels.

It has been proposed that during K channel gating generally, there is a rotation in the transmembrane domains that occur following the pore region(s) (Jiang *et al,* 2002). The mutations seen in this study in the TM4 region of TASK3 (A237T, G236R) might be anticipated to interfere with gating of the channel by altering movement of this TM4 region. This could result in either an interaction with the bundle crossing region of the channel which is in close proximity to this region, or, perhaps more likely, interference with transduction of the regulatory signal from the intracellular regulatory components to the gating region at the selectivity filter via TM4, as seen for TREK1 channels (Bagriantsev *et al,* 2011, 2012).

Pharmacological and genetic recovery of TASK3 current. The TASK3 gain of function mutation (A237T) can overcome some of the effect of the G236R mutation in terms of current density. Indeed in raised extracellular K (25 mM) currents are restored to WT TASK3 levels when measured at -80 mV. However the A237T mutation does not alter the degree of inward rectification, nor does it overcome the influence of G236R on regulation by M3 muscarinic receptors and extracellular acidification. In addition to genetic recovery, it is also possible to overcome the effects of G236R on current density (but not inward rectification) pharmacologically through the use of FFA.

There are precedents for overcoming the effects of mutations in ion channels using pharmacological means. For example, mutations in hERG channels cause long QT syndrome and some trafficking-defective mutants can be rescued by pharmacological agents (Robertson and January, 2006) such as the HERG channel blocking drug E-4031 (Gong *et al,* 2004). Recently, it has been observed that loss of function mutations in TASK1 channels lead to pulmonary arterial hypertension (Ma *et al,* 2013). Some of these mutations can be rescued, experimentally, through up-regulation of TASK1 channel activity by the phospholipase A2 inhibitor ONO-RS-082 (Ma *et al,* 2013).

TASK3 in neuronal development. A reduction in TASK3 channel activity alters both neuronal activity and neuronal development. In TASK3 knockout mice, cerebellar granule neurons are depolarized and their action potential generation is impaired. Thus, TASK3 channels have an important role both in regulating membrane potential and in action potential repolarization, since, in the absence of TASK3 channels, granule neurons could not

Molecular Pharmacology Fast Forward. Published on December 16, 2013 as DOI: 10.1124/mol.113.090530
This article has not been copyedited and formatted. The final version may differ from this version.

maintain sustained repetitive firing (Brickley *et al,* 2007). Knock-down of TASK3 channels (or replacing them with mutated TASK3 channels such as TASK3_G236R channels) altered migration of developing cortical pyramidal neurons (Bando *et al,* 2012). Since this G236R mutation of TASK3 is responsible for Birk Barel mental retardation dysmorphism syndrome (Barel *et al,* 2008), the migration defect caused by dysfunctional TASK3 channels may contribute to the resulting developmental disorders. We have shown that both genetic (a gain of function mutation) and pharmacological (enhancement of current by FFA) interventions can reverse the effect of this mutation on current density. Pharmacological enhancement of TASK3 current during development may, therefore, provide a potentially useful therapeutic strategy in the treatment of Birk Barel syndrome, providing that it is TASK3 current density, *per se,* that is important for channel function in developing neurons.

Authorship Contributions

Participated in research design: Mathie and Veale
Conducted experiments: Veale, Hassan, Walsh and Al-Moubarak
Performed data analysis: Veale, Hassan, Mathie
Wrote or contributed to the writing of the manuscript: Mathie, Veale

Molecular Pharmacology Fast Forward. Published on December 16, 2013 as DOI: 10.1124/mol.113.090530
This article has not been copyedited and formatted. The final version may differ from this version.

References

Alam A and Jiang Y (2009) High-resolution structure of the open NaK channel. *Nat Struct Mol Biol* **16:** 30-34.

Aller MI, Veale EL, Linden AM, Sandu C, Schwaninger M, Evans LJ, Korpi ER, Mathie A, Wisden W, and Brickley SG (2007) Modifying the subunit composition of TASK channels alters the modulation of a leak conductance in cerebellar granule neurons. *J Neurosci* **25:** 11455–11467.

Ashmole I, Vavoulis DV, Stansfeld PJ, Mehta PR, Feng JF, Sutcliffe MJ, and Stanfield PR (2009) The response of the tandem pore potassium channel TASK-3 (K(2P)9.1) to voltage: gating at the cytoplasmic mouth. *J Physiol* **587**: 4769-4783.

Bagriantsev SN, Clark KA, and Minor DL Jr (2012) Metabolic and thermal stimuli control K(2P)2.1 (TREK-1) through modular sensory and gating domains. *EMBO J* **31:** 3297-3308.

Bagriantsev SN, Peyronnet R, Clark KA, Honore E, and Minor DL Jr (2011) Multiple modalities converge on a common gate to control K2P channel function. *EMBO J* **30:** 3594-3606.

Bando Y, Hirano T, and Tagawa Y (2012) Dysfunction of KCNK Potassium Channels Impairs Neuronal Migration in the Developing Mouse Cerebral Cortex. *Cereb Cortex.* doi: 10.1093/cercor/bhs387.

Bandulik S, Tauber P, Penton D, Schweda F, Tegtmeier I, Sterner C, Lalli E, Lesage F, Hartmann M, Barhanin J, and Warth R (2013) Severe hyperaldosteronism in neonatal task3 potassium channel knockout mice is associated with activation of the intraadrenal Renin-Angiotensin system. *Endocrinology* **154:** 2712-2722.

Barel O, Shalev SA, Ofir R, Cohen A, Zlotogora J, Shorer Z, Mazor G, Finer G, Khateeb S, Zilberberg N, and Birk OS (2008) Maternally inherited Birk Barel mental retardation dysmorphism syndrome caused by a mutation in the genomically imprinted potassium channel KCNK9. *Am J Hum Genet* **83:** 193–199.

Ben-Abu Y, Zhou Y, Zilberberg N, and Yifrach O (2009) Inverse coupling in leak and voltage-activated K+ channel gates underlies distinct roles in electrical signalling. *Nat Struct Mol Biol* **16:** 71-79.

Brickley SG, Aller MI, Sandu C, Veale EL, Alder FG, Sambi H*,* Mathie A, and Wisden W (2007) TASK-3 two-pore domain potassium channels enable sustained high-frequency firing in cerebellar granule neurons. *J Neurosci* **27:** 9329-9340.

Brohawn SG, del Marmol J, and MacKinnon R (2012) Crystal structure of the human K2P TRAAK, a lipid- and mechano-sensitive K+ ion channel. *Science* **335:** 436–441.

Clarke CE, Veale EL, Green PJ, Meadows HJ, and Mathie A (2004) Selective block of the human 2-P domain potassium channel, TASK-3, and the native leak potassium current, IK_{SO}, by zinc. *J Physiol* **560:** 51-62.

Clarke CE, Veale EL, Wyse K, Vandenberg JI, and Mathie A. (2008) The M1P1 loop of TASK3 K2P channels apposes the selectivity filter and influences channel function. *J Biol Chem* **283:** 16985–16992

Cohen A, Ben-Abu Y, and Zilberberg N (2009) Gating the pore of potassium leak channels. *Eur Biophys J* **39:** 61-73.

Czirjak G and Enyedi P (2003) Ruthenium red inhibits TASK-3 potassium channel by interconnecting glutamate 70 of the two subunits. *Mol Pharmacol* **63:** 646-652.

Davies LA, Hu C, Guagliardo NA, Sen N, Chen X, Talley EM, Carey RM, Bayliss DA, and Barrett PQ (2008) TASK channel deletion in mice causes primary hyperaldosteronism. *Proc Natl Acad Sci USA* **105:** 2203–2208.

De la Cruz IP, Levin JZ, Cummins C, Anderson P, and Horvitz HR (2003) Sup-9, sup-10, and unc-93 may encode components of a two-pore K_ channel that coordinates muscle contraction in *Caenorhabditis elegans*. *J Neurosci* **23:** 9133–9145.

Duprat F, Lesage F, Fink M, Reyes R, Heurteaux C, and Lazdunski M (1997) TASK, a human background K^+ channel to sense external pH variations near physiological pH. *EMBO J* **16:** 5464-5471.

Ehling P, Bittner S, Bobak N, Schwarz T, Wiendl H, Budde T, Kleinschnitz C, and Meuth SG (2010) Two pore domain potassium channels in cerebral ischemia: a focus on K2P9.1 (TASK3, KCNK9). *Exp Transl Stroke Med* **2:**14.

Enyedi P and Czirjak G (2010) Molecular background of leak K^+ currents: Two-pore domain potassium channels. *Physiol Rev* **90:** 559-605.

Goldstein SA, Bayliss DA, Kim D, Lesage F, Plant LD and Rajan S (2005) International union of pharmacology. LV. Nomenclature and molecular relationships of two-P potassium channels. *Pharmacol Rev* **57:** 527-540.

Gong Q, Anderson CL, January CT, and Zhou Z (2004) Pharmacological rescue of trafficking defective HERG channels formed by coassembly of wild-type and long QT mutant N470D subunits. *Am J Physiol Heart Circ Physiol* **287**: H652-H658.

González W, Zúñiga L, Cid LP, Arévalo B, Niemeyer MI, and Sepúlveda FV (2013) An extracellular ion pathway plays a central role in the cooperative gating of a K(2P) K^+ channel by extracellular pH. *J Biol Chem* **288:** 5984-5991.

Guagliardo NA, Yao J, Hu C, Schertz EM, Tyson DA, Carey RM, Bayliss DA, and Barrett PQ (2012) TASK-3 channel deletion in mice recapitulates low-renin essential hypertension. *Hypertension* **59:** 999-1005.

Hibino H, Inanobe A, Furutani K, Murakami S, Findlay I, and Kurachi Y (2010) Inwardly rectifying potassium channels: their structure, function, and physiological roles. *Physiol Rev* **90:** 291-366.

Higgins DG, Thompson JD, and Gibson TJ (1996) Using CLUSTAL for multiple sequence alignments. *Methods Enzymol* **266:** 383–402.

Jiang Y, Lee A, Chen J, Cadene M, Chait BT, and MacKinnon R (2002) The open pore conformation of potassium channels. *Nature* **417:** 523-526.

Molecular Pharmacology Fast Forward. Published on December 16, 2013 as DOI: 10.1124/mol.113.090530
This article has not been copyedited and formatted. The final version may differ from this version.

Kananura C, Sander T, Rajan S, Preisig-Muller R, Grzeschik KH, Daut J, Derst C, and Steinlein OK (2002) Tandem pore domain K- channel TASK-3 (KCNK9) and idiopathic absence epilepsies. *Am J Med Genet* **114:** 227–229.

Kim Y, Bang H, and Kim D (2000) TASK-3, a new member of the tandem pore K^+ channel family. *J Biol Chem* **275:** 9340-9347.

Li W and Aldrich RW (2011) Electrostatic influences of charged inner pore residues on the conductance and gating of small conductance Ca^{2+} activated K^+ channels. *Proc Natl Acad Sci U S A* **108:** 5946-5953.

Linden AM, Sandu C, Aller MI, Vekovischeva OY, Rosenberg PH, Wisden W, and Korpi ER (2007) TASK-3 knockout mice exhibit exaggerated nocturnal activity, impairments in cognitive functions, and reduced sensitivity to inhalation anesthetics. *J Pharmacol Exp Ther* **323:** 924-934.

Luedi PP, Dietrich FS, Weidman JR, Bosko JM, Jirtle RL, and Hartemink AJ (2007) Computational and experimental identification of novel human imprinted genes. *GenomeRes* **17:** 1723–1730.

Ma L, Roman-Campos D, Austin ED, Eyries M, Sampson KS, Soubrier F, Germain M, Trégouët DA, Borczuk A, Rosenzweig EB, Girerd B, Montani D, Humbert M, Loyd JE, Kass RS, and Chung WK (2013) A novel channelopathy in pulmonary arterial hypertension. *N Engl J Med* **369:** 351-361.

Ma L, Zhang X, Zhou M, and Chen H (2012) Acid-sensitive TWIK and TASK two-pore domain potassium channels change ion selectivity and become permeable to sodium in extracellular acidification. *J Biol Chem* **287:** 37145-37153.

Mathie A, Al-Moubarak E, and Veale EL (2010) Gating of two pore domain potassium channels. *J Physiol* **588:** 3149-3156.

Millar JA, Barratt L, Southan AP, Page KM, Fyffe REW, Robertson B, and Mathie A (2000) A functional role for the two-pore domain potassium channel TASK-1 in cerebellar granule neurons. *Proc Natl Acad Sci USA* **97:** 3614–3618.

Morton MJ, Chipperfield S, Abohamed A, Sivaprasadarao A, and Hunter M. (2005) Na^+-induced inward rectification in the two-pore domain K^+ channel, TASK-2. *Am J Physiol Renal Physiol* **288:** F162-169

Mu D, Chen L, Zhang X, See LH, Koch CM, Yen C*,* Tong JJ, Spiegel L, Nguyen KC, Servoss A, Peng Y, Pei L, Marks JR, Lowe S, Hoey T, Jan LY, McCombie WR, Wigler MH, and Powers S. (2003) Genomic amplification and oncogenic properties of the KCNK9 potassium channel gene. *Cancer Cell* **3:** 297-302.

Patel AJ, Maingret F, Magnone V, Fosset M, Lazdunski M, and Honore E (2000) TWIK2, an inactivating domain K^+ channel. *J Biol Chem* **275:** 28722–28730.

Pei L, Wiser O, Slavin A, Mu D, Powers S, Jan LY, and Hoey T (2003) Oncogenic potential of TASK3 (Kcnk9) depends on K^+ channel function. *Proc Natl Acad Sci U S A* **100:** 7803-7807.

Penton D, Bandulik S, Schweda F, Haubs S, Tauber P, Reichold M, Cong LD, El Wakil A, Budde T, Lesage F, Lalli E, Zennaro MC, Warth R, and Barhanin J (2012) Task3 potassium

channel gene invalidation causes low renin and salt-sensitive arterial hypertension. *Endocrinology* **153:** 4740-4748.

Piechotta PL, Rapedius M, Stansfeld PJ, Bollepalli MK, Erhlich G, Andres-Enguix I, Fritzenshaft H, Decher N, Sansom MS, Tucker SJ, and Baukrowitz T (2011) The pore structure and gating mechanism of K2P channels *EMBO J* **30:** 3607-3619.

Rajan S, Wischmeyer E, Xin Liu G, Preisig-Muller R, Daut J, Karschin A, and Derst C (2000) TASK-3, a novel tandem pore domain acid-sensitive K^+ channel. An extracellular histiding as pH sensor. *J Biol Chem* **275:**16650-16657.

Robertson GA and January CT (2006) HERG trafficking and pharmacological rescue of LQTS-2 mutant channels. *Handb Exp Pharmacol* **171:** 349-55.

Sali A and Blundell TL (1993) Comparative protein modelling by satisfaction of spatial restraints. *J Mol Biol* **234:** 779-815.

Takahira M, Sakurai M, Sakurada N, and Sugiyama K (2005) Fenamates and diltiazem modulate lipid-sensitive mechano-gated 2P domain K(+) channels. *Pflugers Arch* **451(3):** 474-478.

Talley EM, Solorzano G, Lei Q, Kim D and Bayliss DA (2001) Cns distribution of members of the two-pore-domain (KCNK) potassium channel family. *J Neurosci* **21:** 7491-7505.

Veale EL, Buswell R, Clarke CE, and Mathie A (2007a) Identification of a region in the TASK3 two pore domain potassium channel that is critical for its blockade by methanandamide. *Br J Pharmacol* **152:** 778-786.

Veale EL, Kennard LE, Sutton GL., MacKenzie G, Sandu C, and Mathie A (2007b) G(alpha)q-mediated regulation of TASK3 two-pore domain potassium channels: The role of protein kinase C. *Mol Pharmacol* **71:** 1666-1675.

Watkins CS and Mathie A (1996) A non-inactivating K+ current sensitive to muscarinic receptor activation in rat cultured cerebellar granule neurons. *J Physiol* **491:** 401-412.

Footnotes

AM is a Royal Society Industry Fellow [Grant IF080012/AM]. Supported by the Biotechnology and Biological Sciences Rresearch Council [Grant BB/J000930/1].

Molecular Pharmacology Fast Forward. Published on December 16, 2013 as DOI: 10.1124/mol.113.090530
This article has not been copyedited and formatted. The final version may differ from this version.

Figure Legends

Figure 1. Characteristics of currents through wild type TASK3 and TASK3_G236R channels. *A*, Histogram of outward current densities measured as the difference current between that at -40 mV and -80 mV for WT TASK3 and TASK3_G236R channels in normal (2.5 mM K) external (*** = $p < 0.001$, t-test). *B*, Histogram of inward current densities measured at -120 mV for WT TASK3 and TASK3_G236R channels in normal (2.5 mM K) external. *C*, plot of reversal potential versus external K concentration for WT TASK3 (red squares) and TASK3_G236R (blue triangles). The solid line represents a pure K conductance. *D-F*, Currents recorded through WT TASK3 channels in 2.5 and 147.5 mM external K (blue) and 147.5 mM external Rb (orange). Currents were evoked by the standard "step-ramp" voltage protocol as detailed in Materials and Methods. Insets show current-voltage relationships. *G-I*, Currents evoked by the step-ramp voltage protocol recorded through TASK3_G236R channels in 2.5 and 147.5 mM external K (blue) and 147.5 mM external Rb (orange). Insets show current-voltage relationships. Note the clear inward rectification seen for TASK3_G236R mutated channels in all three external solutions.

Figure 2. Homology model of human TASK3 channel. Model of hTASK3 based on TRAAK crystal structure. For clarity, TM3 (M3) and TM4 (M4) are rotated through 90^{o} and separated from TM1 (M1) and TM2 (M2). Positively charged amino acids are in blue and negatively charged amino acids in red. G236R in TM4 is highlighted by the arrow and adds a positively charged amino acid to the intracellular cavity of the pore. The adjacent amino acid A237 is indicated in green. Mutation A237T is a gain of function mutation.

Figure 3. Recovery of current through TASK3_G236R channels by TASK3_A237T gain of function mutation. *A*, Histogram of outward current densities measured as the difference current between that at -40 mV and -80 mV for WT TASK3, TASK3_G236R and TASK3_G236R_A237T channels in normal (2.5 mM K) external, (* = significantly different from wild type at < 0.05 level, ANOVA followed by Tukey's test). *B,* Current-voltage relationship for currents through TASK3_G236R_A237T channels in normal external solution. *C*, Histogram of inward current densities measured at -80 mV for WT TASK3, TASK3_G236R and TASK3_G236R_A237T channels in 25 mM K external, (* = significantly different from wild type at < 0.05 level, ANOVA followed by Dunnett's test). *D*, Current-voltage relationship for currents through G236R_A237T channels in 25 mM K external. *E*, Histogram of inward current densities measured at -80 mV for WT TASK3, TASK3_G236R

Molecular Pharmacology Fast Forward. Published on December 16, 2013 as DOI: 10.1124/mol.113.090530
This article has not been copyedited and formatted. The final version may differ from this version.

and TASK3_G236R_A237T channels in 25 mM Rb external. *F*, Current voltage relationship for currents through TASK3_G236R_A237T channels in 25 mM Rb external.

Figure 4. Inhibition by extracellular acidification (pH 6.4) and zinc (100 μM) is reduced in TASK3_G236R channels. *A*, Histogram of percentage inhibition of current by pH 6.4 for WT TASK3, TASK3_G236R, TASK3_A237T and TASK3_G236R_A237T, (* = significantly different from wild type at < 0.05 level, ANOVA followed by Dunnett's test). *B*, Representative time course for inhibition of outward current by extracellular acidification for current through TASK3_G236R channels. Application of pH 6.4 is indicated by the purple bar. *C*, Histogram of percentage inhibition of current by zinc (100 μM) for WT TASK3, TASK3_G236R, TASK3_A237T and TASK3_G236R_A237T, (* = significantly different from wild type at < 0.05 level, ANOVA followed by Dunnett's test). *D*, Representative time course for inhibition of outward current by zinc (100 μM) for current through TASK3_G236R channels. Application of zinc is indicated by the green bar.

Figure 5. Inhibition of current by muscarine is abolished in TASK3_G236R channels. *A*, Histogram of percentage inhibition of current by 0.1, 1 and 10 μM muscarine for WT TASK3 channels. *B*, Representative time course for inhibition of outward current by muscarine (1 μM) for current through WT TASK3 channels. Application of muscarine is indicated by the blue bar. *C*, Histogram of percentage enhancement of current by 0.1, 1 and 10 μM muscarine for TASK3_G236R channels. *D*, Representative time course for effect on outward current of muscarine (1 μM) for current through TASK3_G236R channels. *E*, Histogram of percentage inhibition of current by 0.1, 1 and 10 μM muscarine for TASK3_A237T channels. *F*, Representative time course for inhibition of outward current by muscarine (1 μM) for current through TASK3_A237T channels.

Figure 6. Enhancement of TASK3_G236R current by FFA. *A*, Histogram of percentage enhancement of current by FFA (100 μM) for WT TASK3, TASK3_G236R, TASK3_A237T and TASK3_G236R_A237T channels, (* = significantly different from wild type at < 0.05 level, ANOVA followed by Dunnett's test). *B*, Representative time course for enhancement of outward current by FFA (100 μM) for current through WT TASK3 channels. Application of FFA is indicated by the red bar. *C*, Currents evoked by the step-ramp voltage protocol recorded through WT TASK3 channels in the absence and presence (red) of FFA (100 μM). *D*, Current-voltage relationships for WT TASK3 channels in the absence and presence (red) of FFA (100 μM). *E–G*, as *B-D* for TASK3_G236R channels. *H–J*, as *B-D* for TASK3_G236R_A237T channels.

Molecular Pharmacology Fast Forward. Published on December 16, 2013 as DOI: 10.1124/mol.113.090530
This article has not been copyedited and formatted. The final version may differ from this version.

Figure 7. Properties and regulation of currents through TASK3 G236F channels. *A*, Histogram of outward current densities measured as the difference current between that at -40 mV and -80 mV for WT and G236F channels in normal (2.5 mM K) external, (*** = $p < 0.001$, t-test). *B*, Histogram of inward current densities measured at -120 mV for WT and G236F channels in normal (2.5 mM K) external, (*** = $p < 0.001$, t-test). *C*, Current-voltage relationship for currents through G236F channels in normal external solution. *D* Histogram of percentage enhancement of current by FFA (100 µM) for WT and G236R channels. *E*, Representative time course for enhancement of outward current by FFA (100 µM) for current through G236F channels. Application of FFA is indicated by the red bar. *F*, Current-voltage relationships for G236F channels in the absence and presence (red) of FFA (100 µM). *G*, Histogram of percentage inhibition of current by muscarine (1 µM) for WT and G236R channels, (*** = $p < 0.001$, t-test). *H,* Representative time course for inhibition of outward current by muscarine (1 µM) for current through G236F channels. Application of muscarine is indicated by the blue bar. *I*, Current-voltage relationships for G236F channels in the absence and presence (blue) of muscarine (1 µM). *J*, Histogram of percentage inhibition of current by pH 6.4 for WT and G236R channels. *K*, Representative time course for inhibition of outward current by pH 6.4 for current through G236F channels. Application of pH 6.4 is indicated by the purple bar. *L*, Current-voltage relationships for G236F channels in the absence and presence (purple) of pH 6.4. *M*, Histogram of percentage inhibition of current by zinc (100 µM) for WT and G236R channels. *N*, Representative time course for inhibition of outward current by zinc (100 µM) for current through G236F channels. Application of zinc is indicated by the green bar. *O*, Current-voltage relationships for G236F channels in the absence and presence (green) of zinc (100 µM).

Figure 1

Molecular Pharmacology Fast Forward. Published on December 16, 2013 as DOI: 10.1124/mol.113.090530
This article has not been copyedited and formatted. The final version may differ from this version.

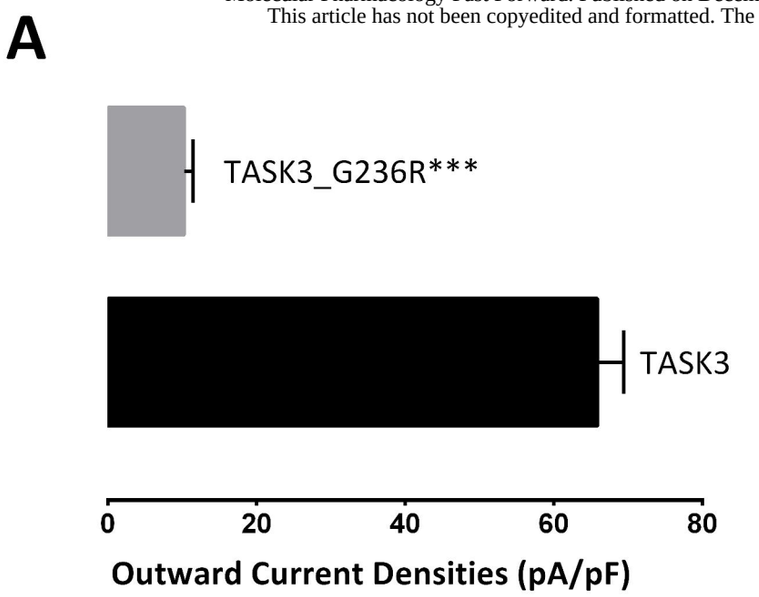

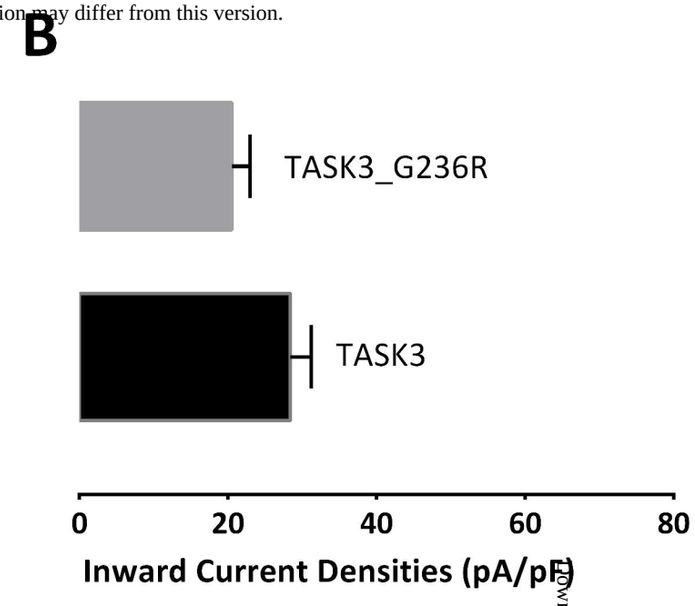

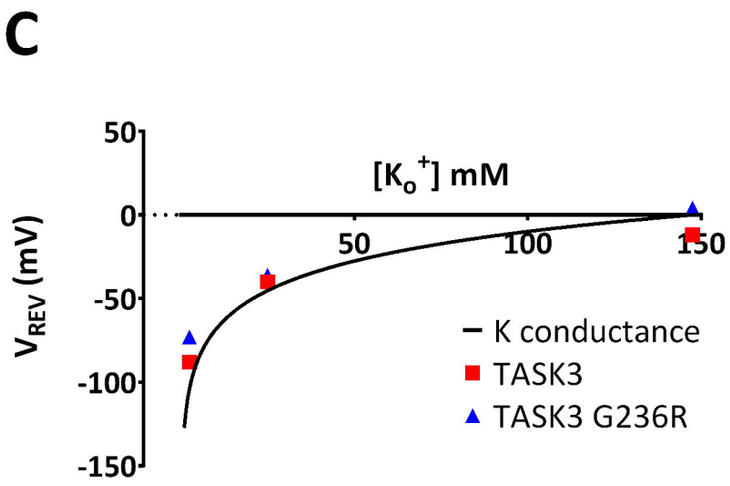

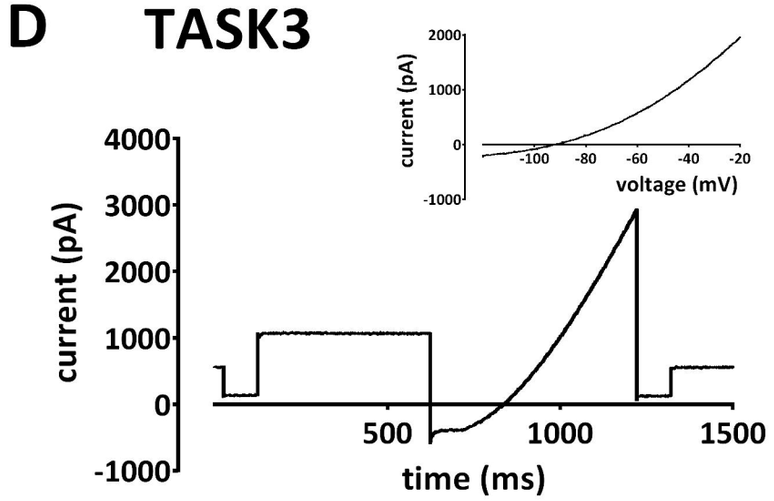

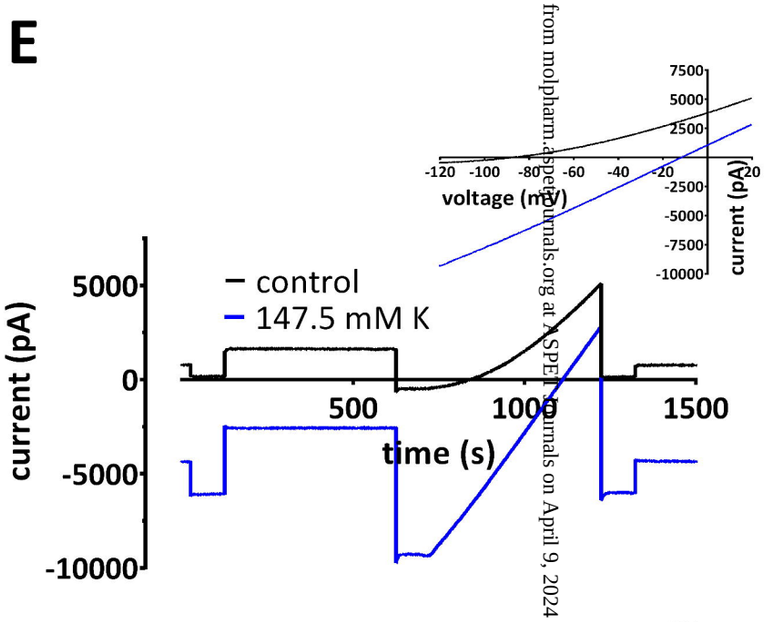

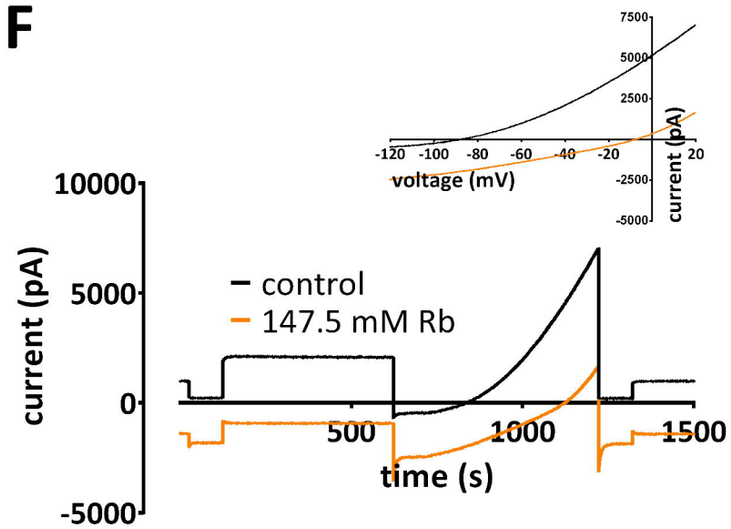

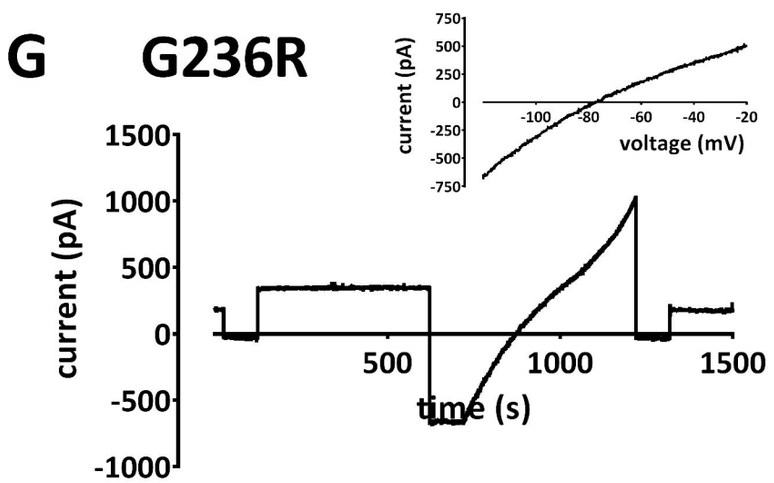

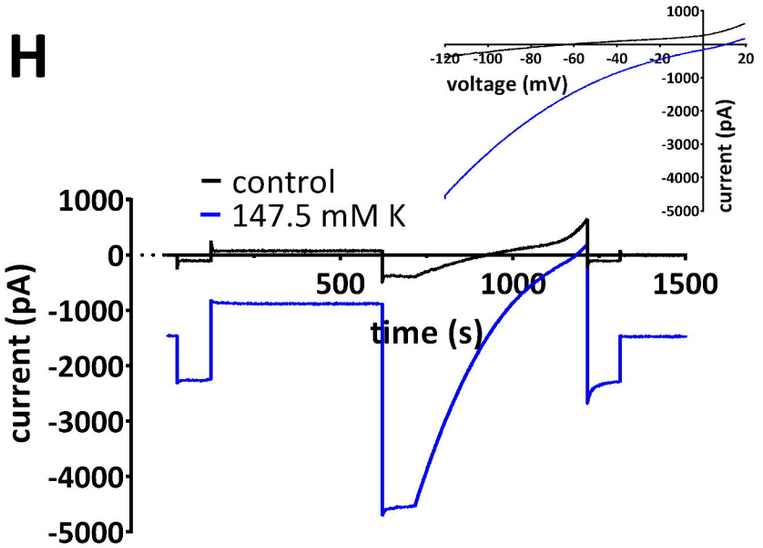

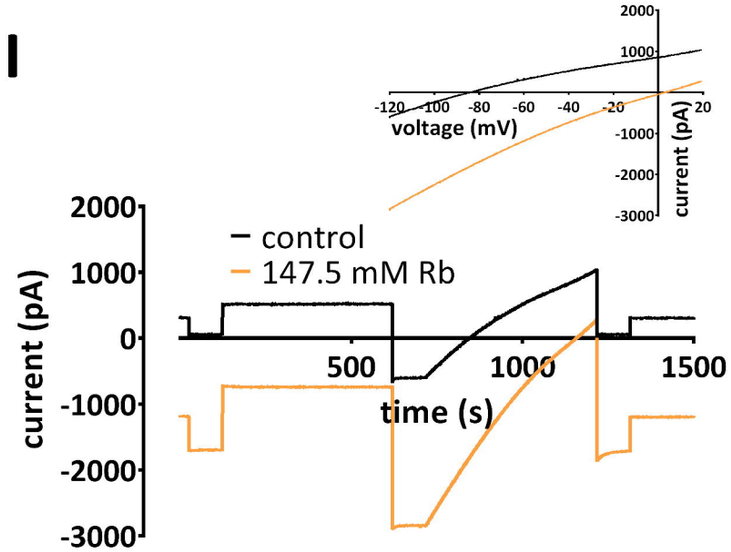

Figure 2

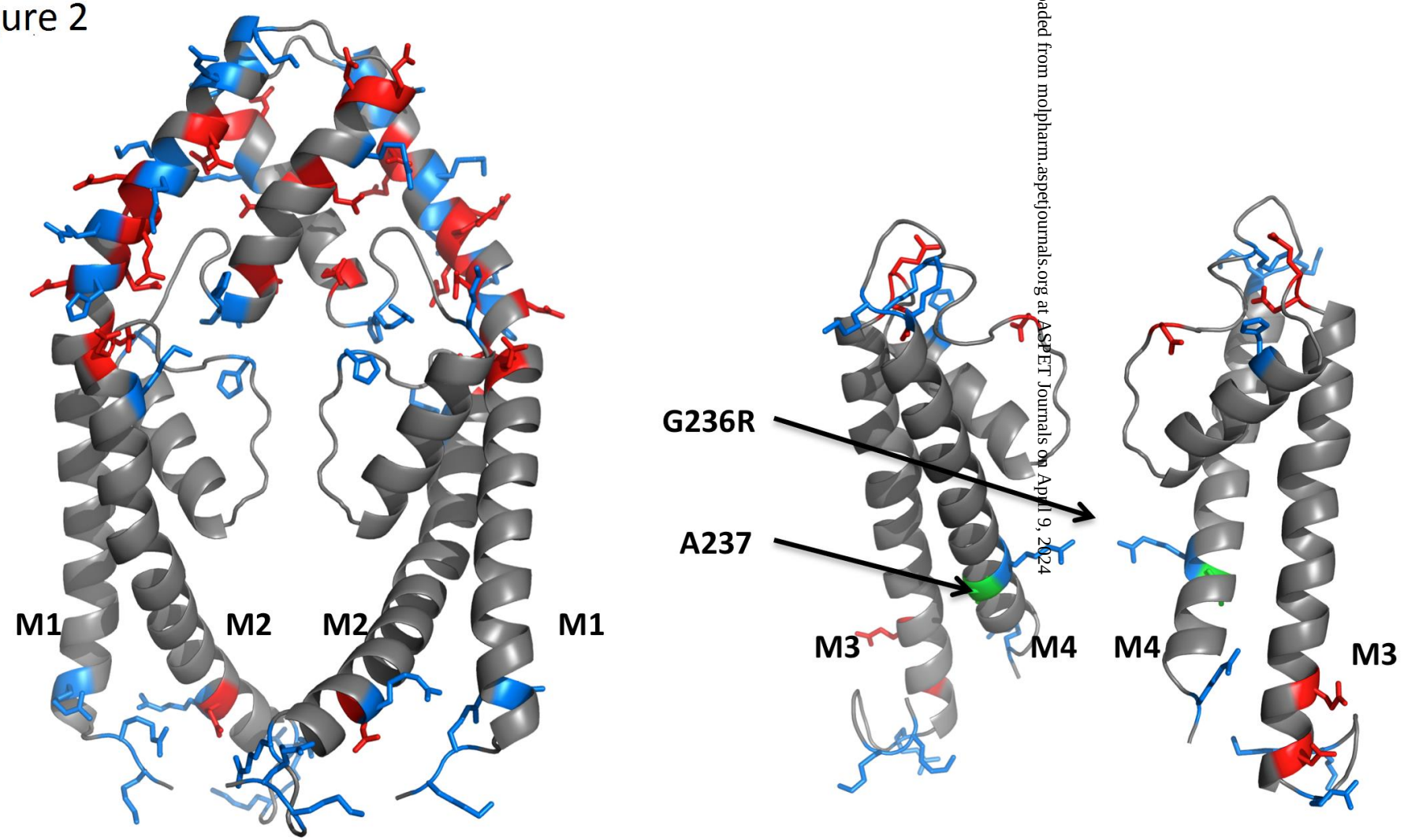

Figure 3

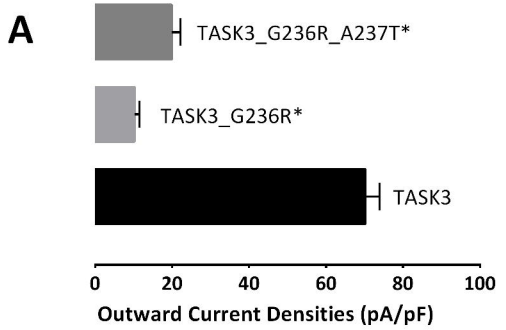
A
TASK3_G236R_A237T*
TASK3_G236R*
TASK3
0
20
40
60
80
100
Outward Current Densities (pA/pF)

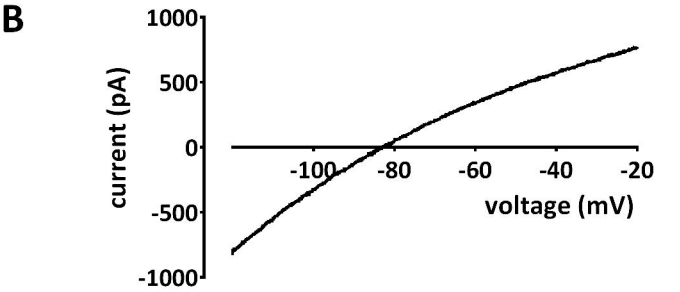
B
1000
500
0
-500
-1000
current (pA)
-100
-80
-60
-40
-20
voltage (mV)

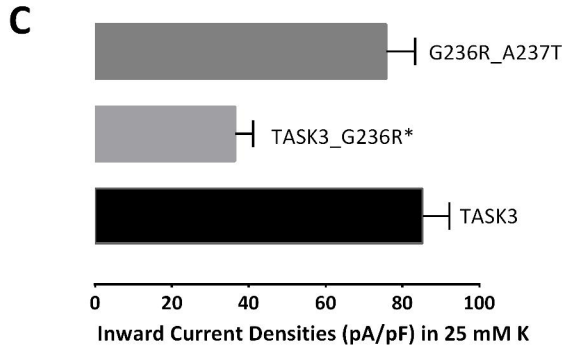
C
G236R_A237T
TASK3_G236R*
TASK3
0
20
40
60
80
100
Inward Current Densities (pA/pF) in 25 mM K

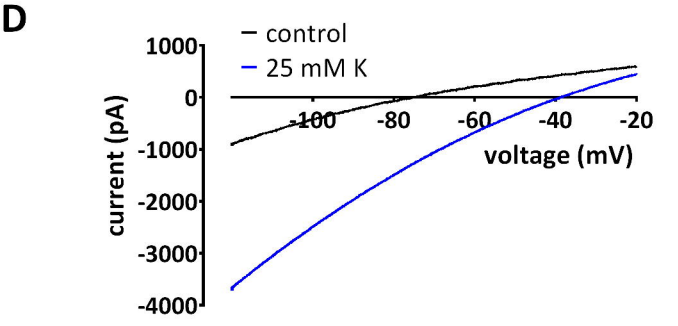
D
control
25 mM K
1000
0
-1000
-2000
-3000
-4000
current (pA)
-100
-80
-60
-40
-20
voltage (mV)

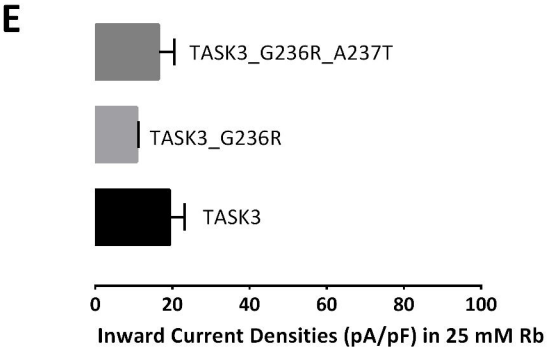
E
TASK3_G236R_A237T
TASK3_G236R
TASK3
0
20
40
60
80
100
Inward Current Densities (pA/pF) in 25 mM Rb

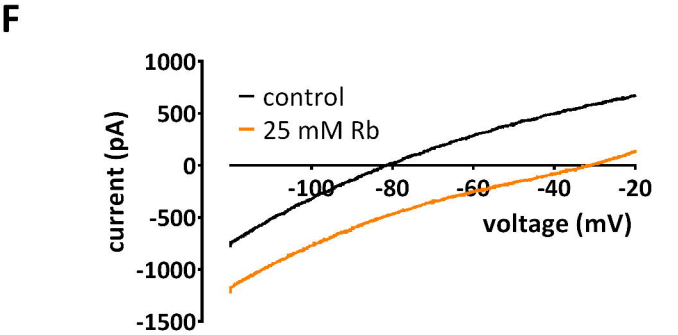
F
1000
500
0
-500
-1000
-1500
current (pA)
control
25 mM Rb
-100
-80
-60
-40
-20
voltage (mV)

Figure 4

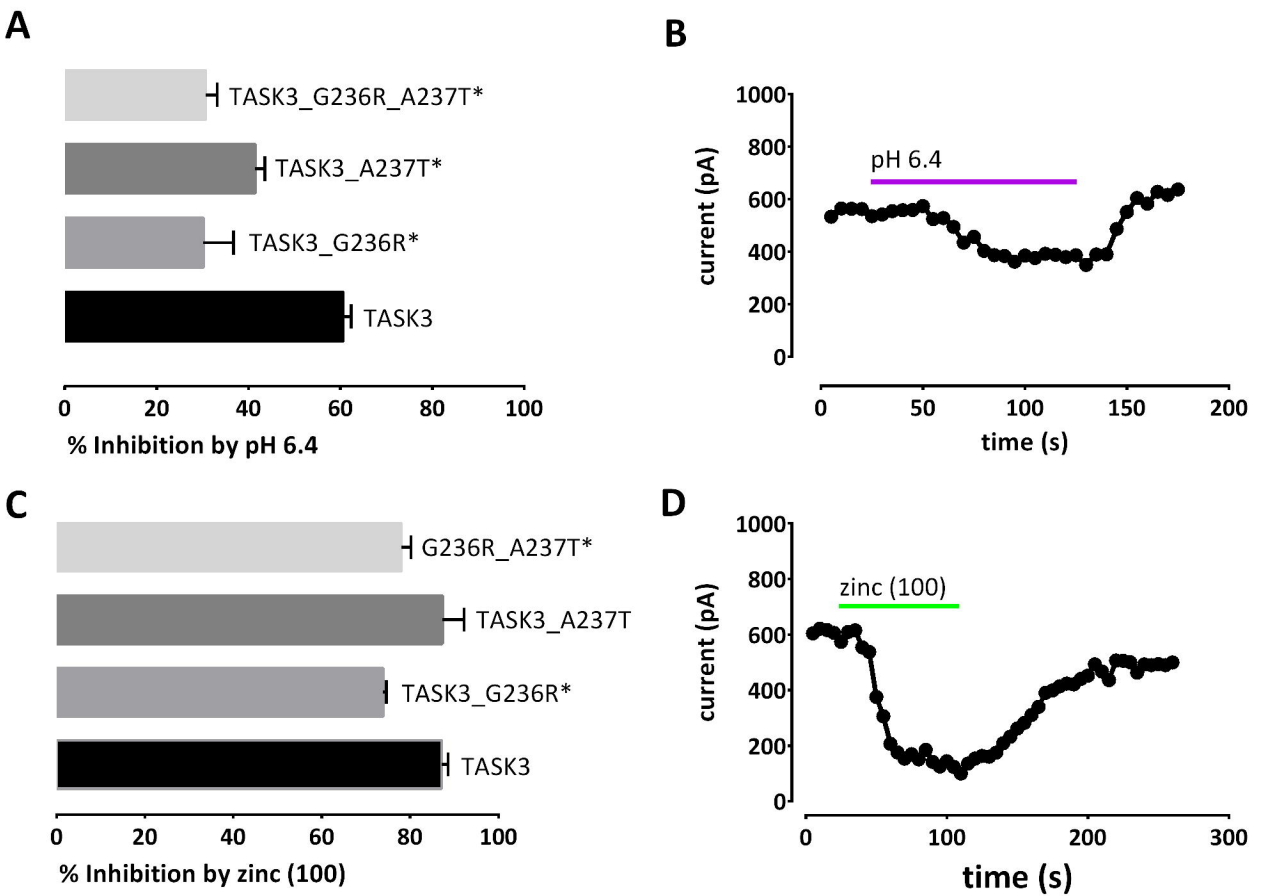
A
TASK3_G236R_A237T*
TASK3_A237T*
TASK3_G236R*
TASK3
0
20
40
60
80
100
% Inhibition by pH 6.4
B
1000
800
600
400
200
0
current (pA)
pH 6.4
0
50
100
150
200
time (s)
C
G236R_A237T*
TASK3_A237T
TASK3_G236R*
TASK3
0
20
40
60
80
100
% Inhibition by zinc (100)
D
1000
800
600
400
200
0
current (pA)
zinc (100)
0
100
200
300
time (s)

Figure 5

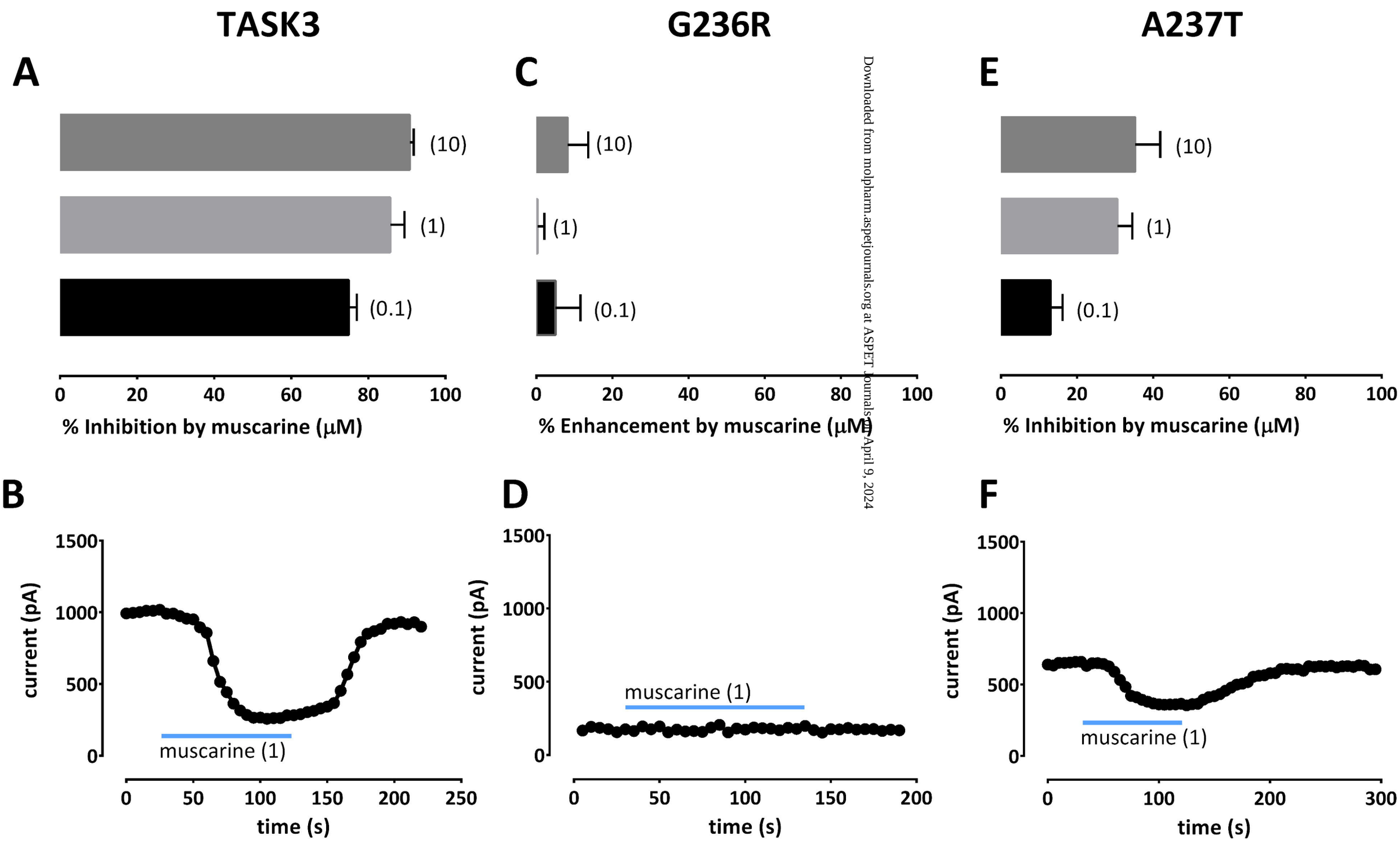

Figure 6

Molecular Pharmacology Fast Forward. Published on December 16, 2013 as DOI: 10.1124/mol.113.090530
This article has not been copyedited and formatted. The final version may differ from this version.

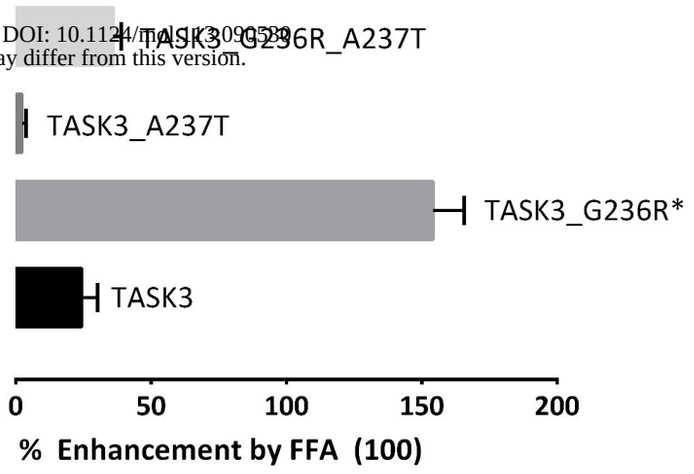

TASK3

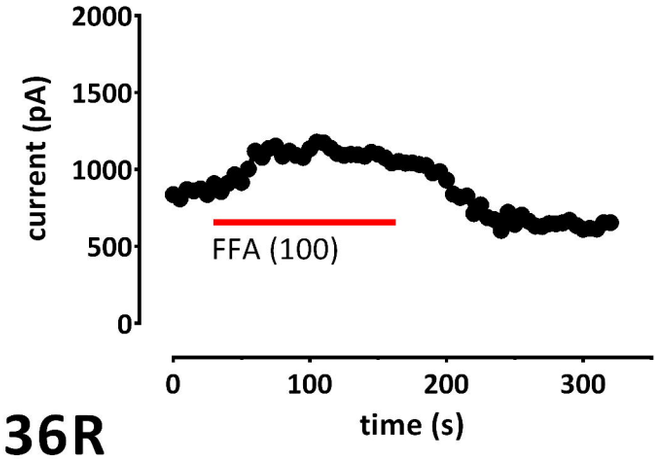

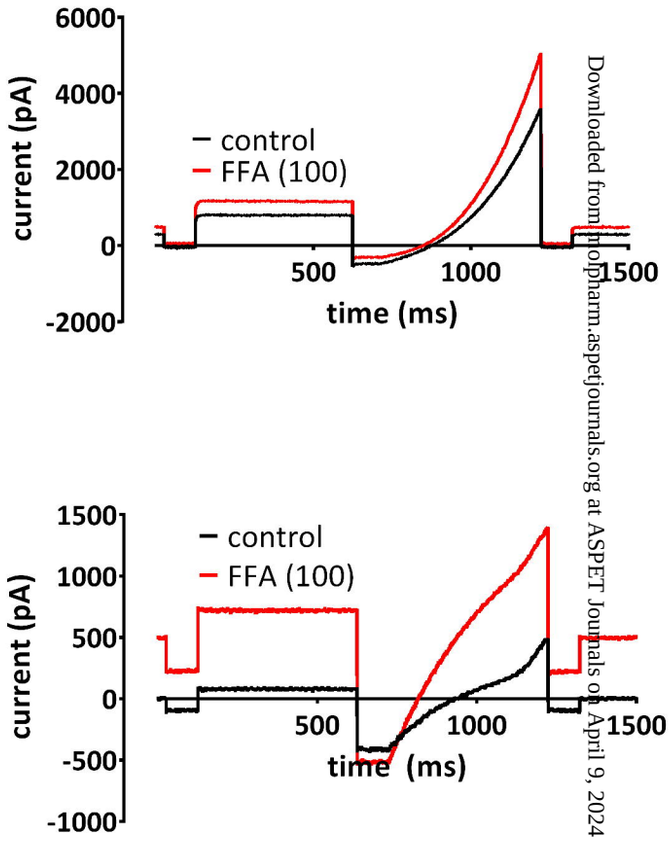

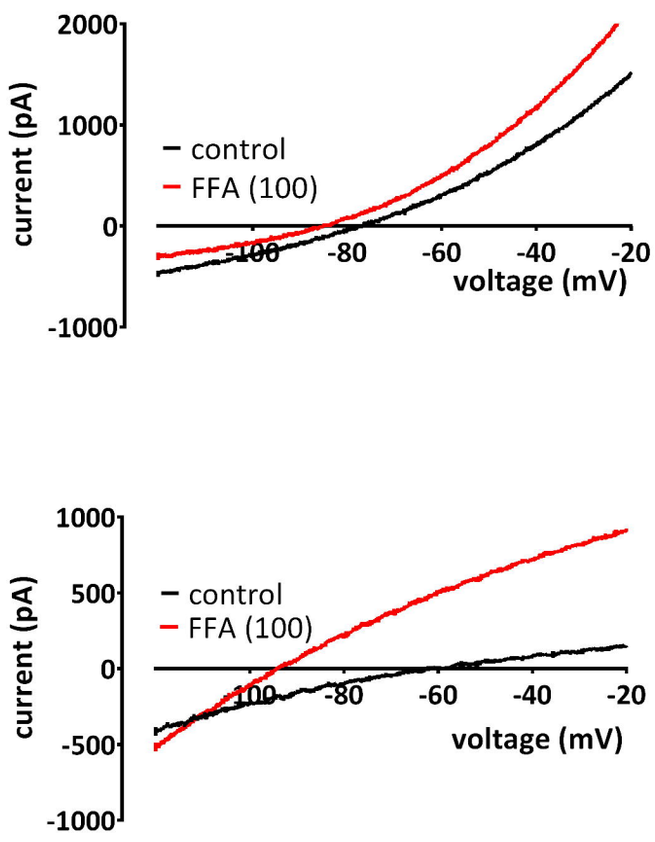

G236R

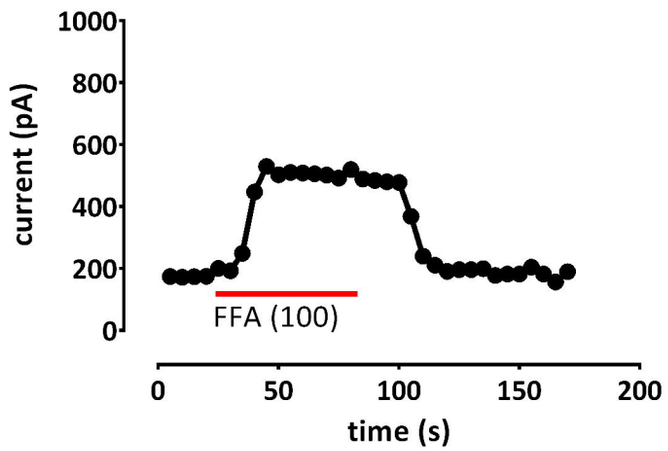

G236R_A237T

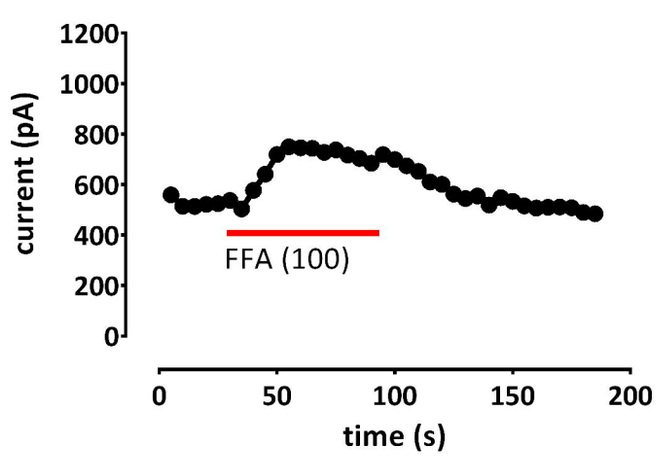

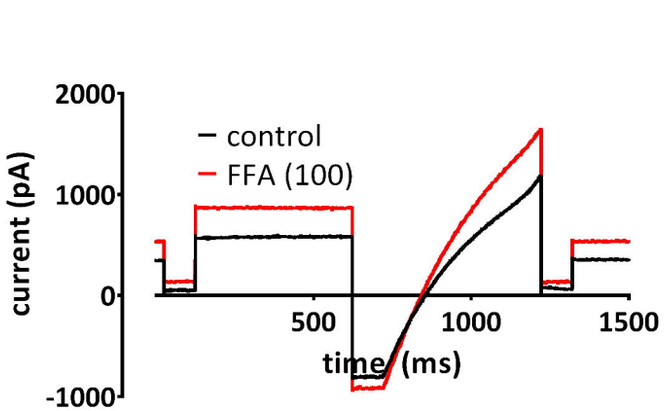

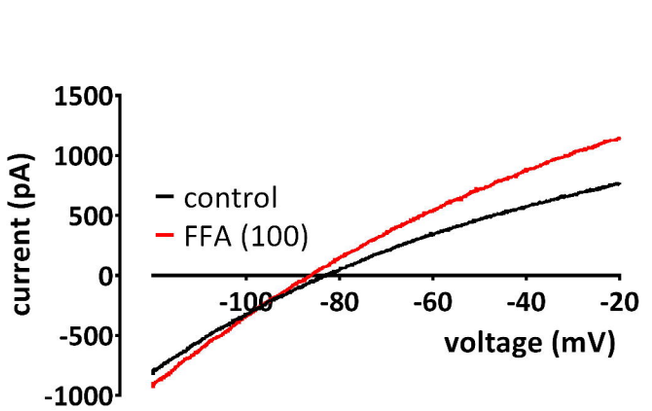

Figure 7

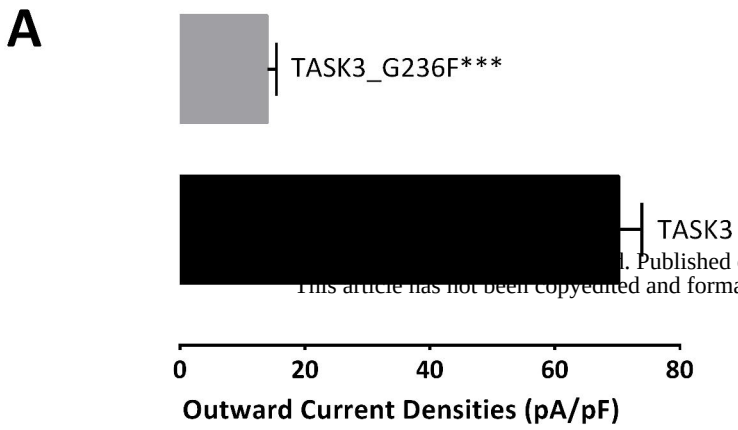

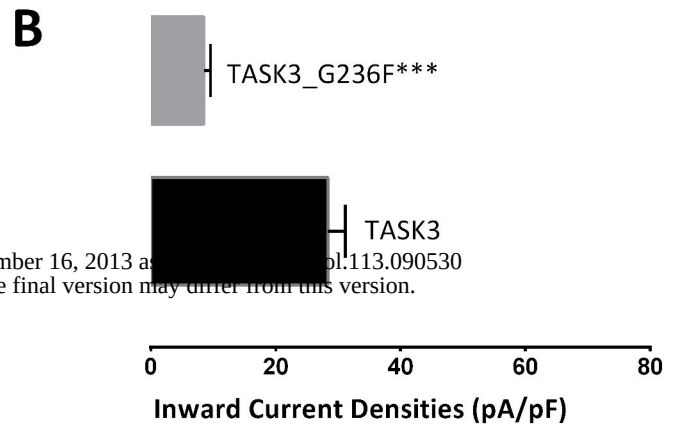

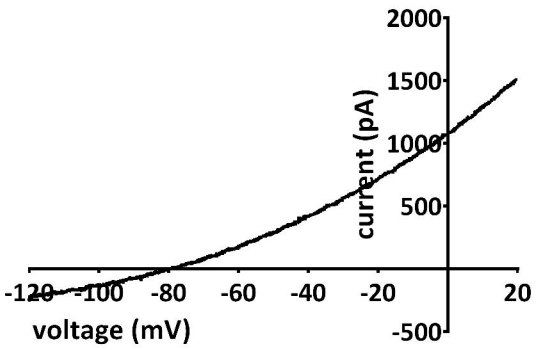

. Published on December 16, 2013 as ol.113.090530

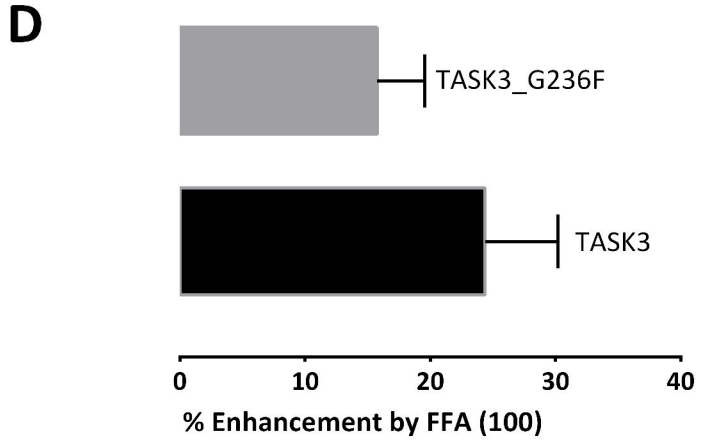

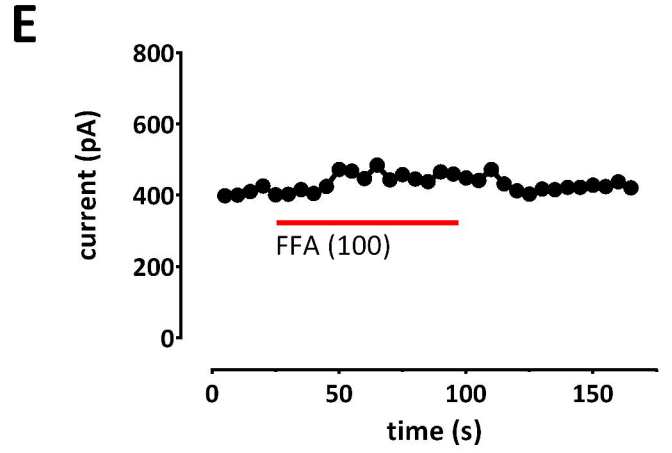

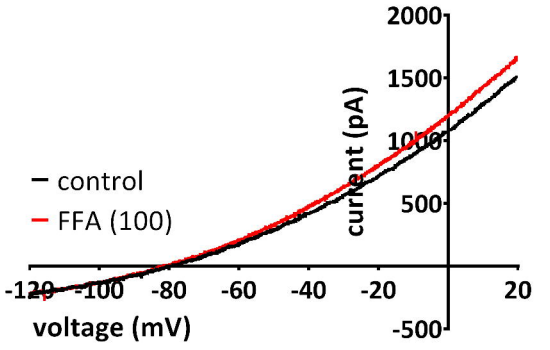

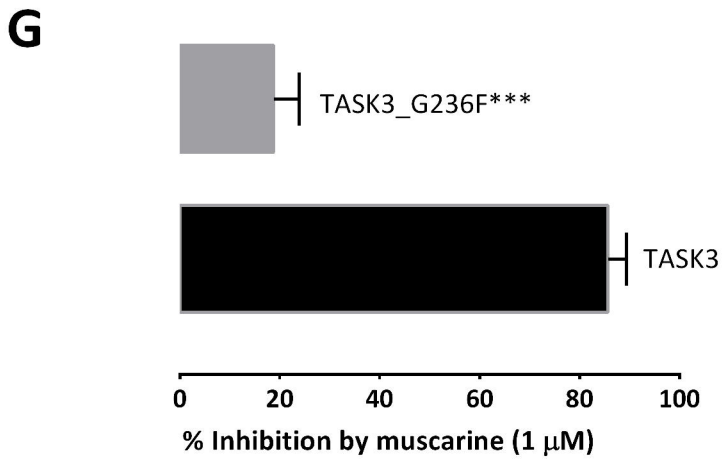

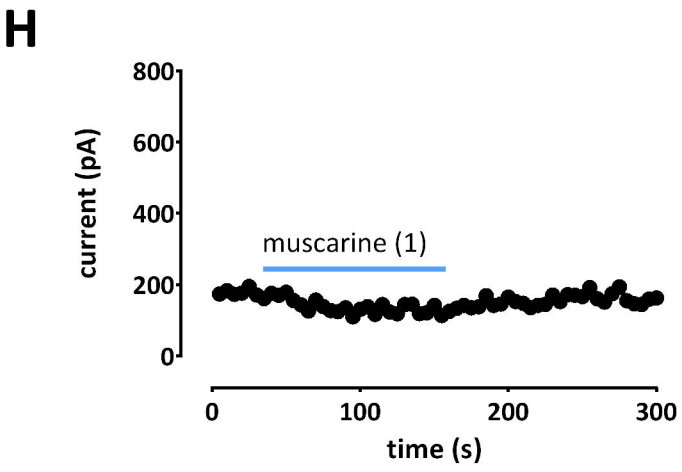

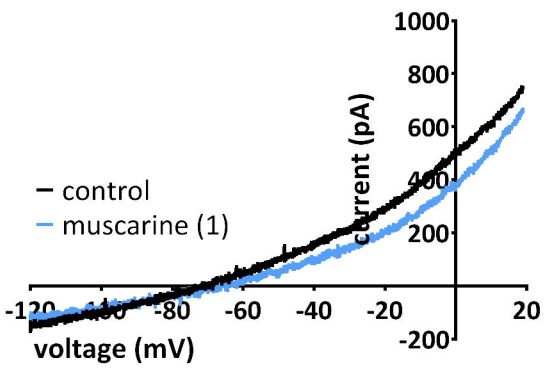

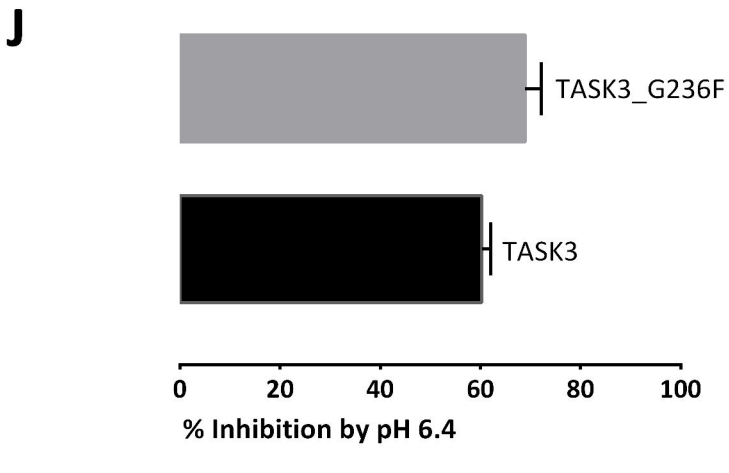

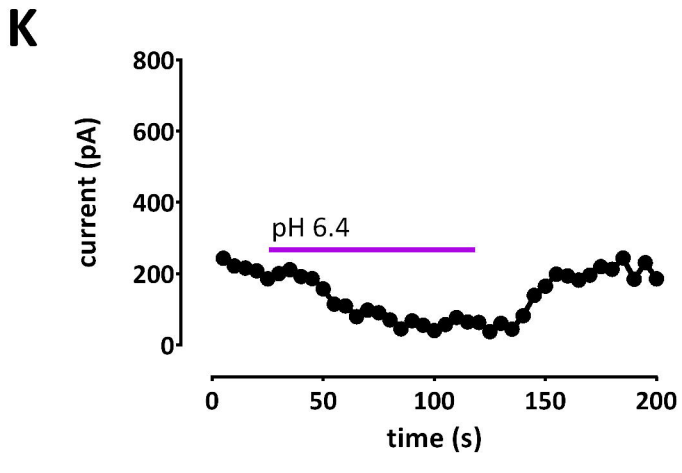

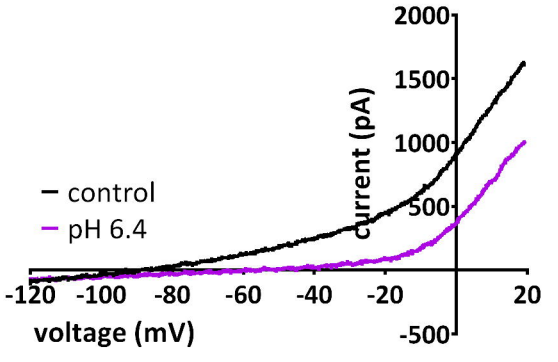

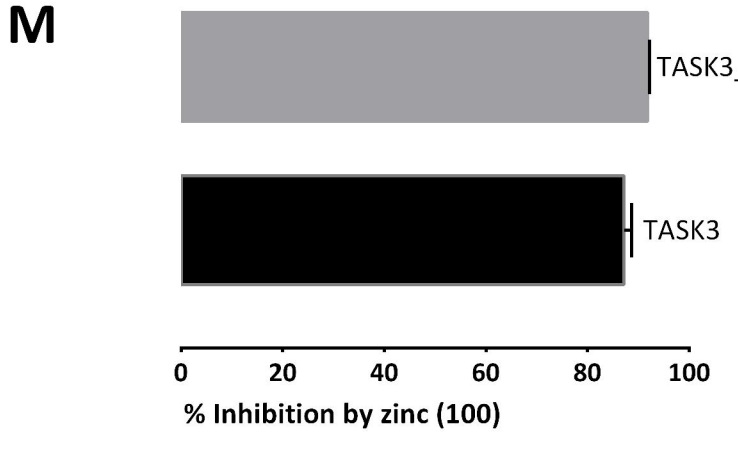

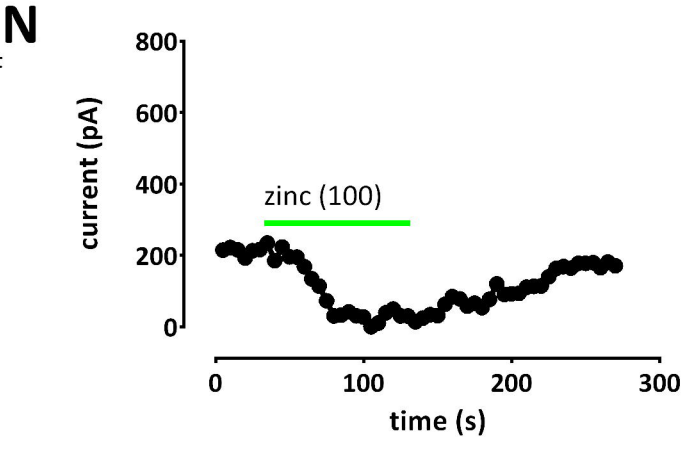

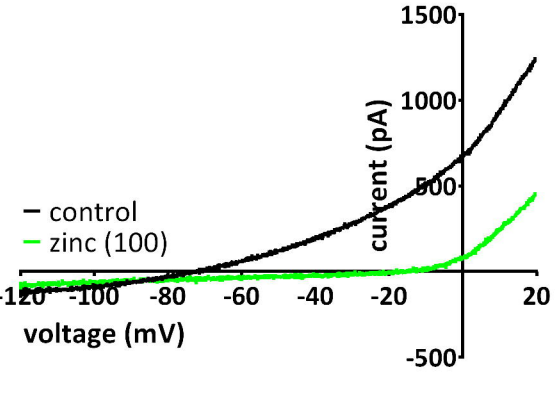

Recovery of current through mutated TASK3 potassium channels underlying Birk Barel syndrome

Emma L Veale, Mustafa Hassan, Yvonne Walsh, Ehab Al-Moubarak, Alistair Mathie

Molecular Pharmacology

Supplementary Information

Supplementary Figure 1. Current in untransfected tsA201 cells is negligible below -20 mV. *A*, Histogram of outward current densities measured as the difference current between that at -40 mV and -80 mV for WT and G236R channels and untransfected cells in normal (2.5 mM K) external, (* = significantly different from wild type at < 0.05 level, ANOVA followed by Tukey's test). *B*, Histogram of inward current densities measured at -80 mV for WT and G236F channels and untransfected cells in 147.5 mM K external, (* = significantly different from wild type at < 0.05 level, ANOVA followed by Tukey's test). *C*, Representative time course for inward current at -80 mV in normal external solution and 147.5 mM K external (blue bar) in untransfected cells. *D*, Currents recorded in untransfected cells in 2.5 and 147.5 mM external K (blue). Currents were evoked by our standard "step-ramp" voltage protocol as detailed in Materials and Methods. Insets show current-voltage relationships.

Supplementary Figure 2. Properties of currents through wild type murine TASK3 and murine TASK3_G236R channels. *A*, Histogram of outward currents measured as the difference current between that at -40 mV and -80 mV for WT and G236R channels in normal (2.5 mM K) external, (*** = $p < 0.001$, t-test). *B*, Currents recorded through WT TASK3 channels in 2.5 mM external K. Currents were evoked by our standard "step-ramp" voltage protocol as detailed in Materials and Methods. *C,* Current-voltage relationship for WT mTASK3 channels. *D*, Currents recorded through mTASK3_G236R channels in 2.5 mM external K. Currents were evoked by our standard "step-ramp" voltage protocol as detailed in Materials and Methods. *E*, Current-voltage relationship for mTASK3_G236R channels. Note the clear inward rectification seen for mTASK3_G236R channels.

Supplementary Figure 3. Homology model of mouse TASK3 channel. Model of mouse TASK3 based on TRAAK crystal structure. For clarity, TM3 (M3) and TM4 (M4) are rotated through 90^{o} and separated from TM1 (M1) and TM2 (M2). Positively charged amino acids are in blue and negatively charged amino acids in red. G236R in TM4 is highlighted by the arrow and adds a positively charged amino acid to the intracellular cavity of the pore. The adjacent amino acid A237 is indicated in green.

Supplementary Figure 1

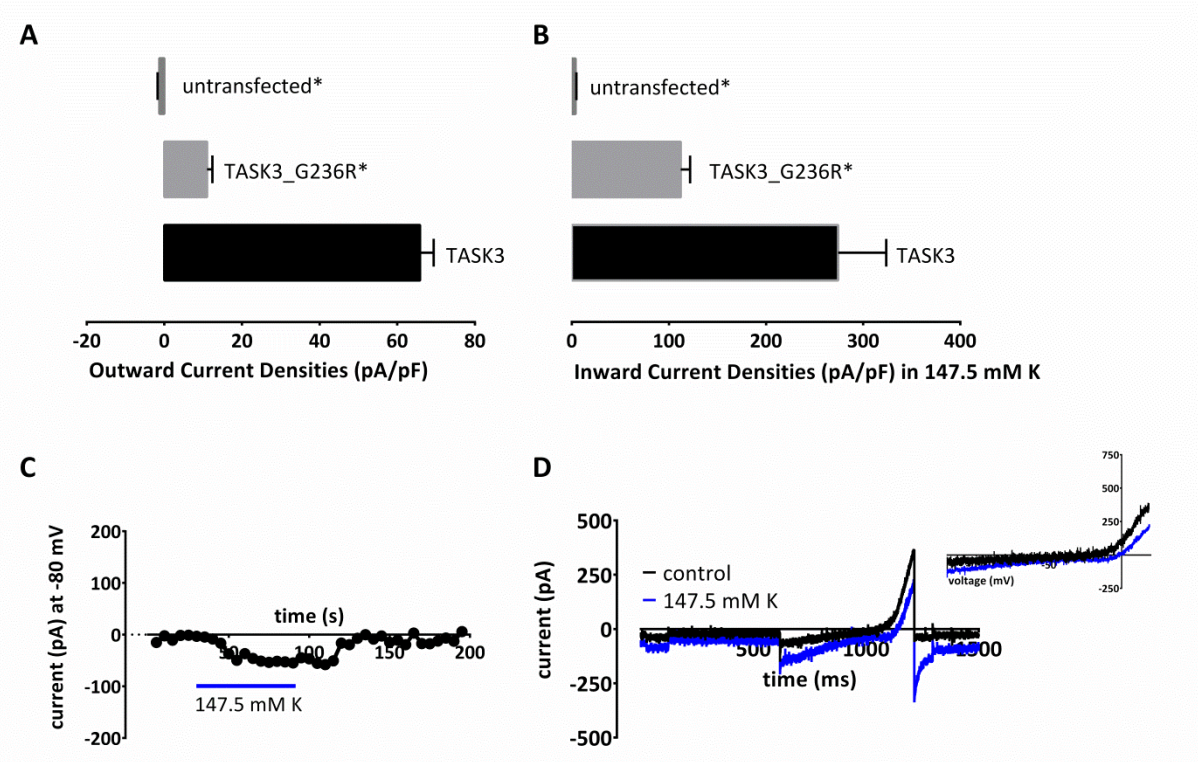

Supplementary Figure 2

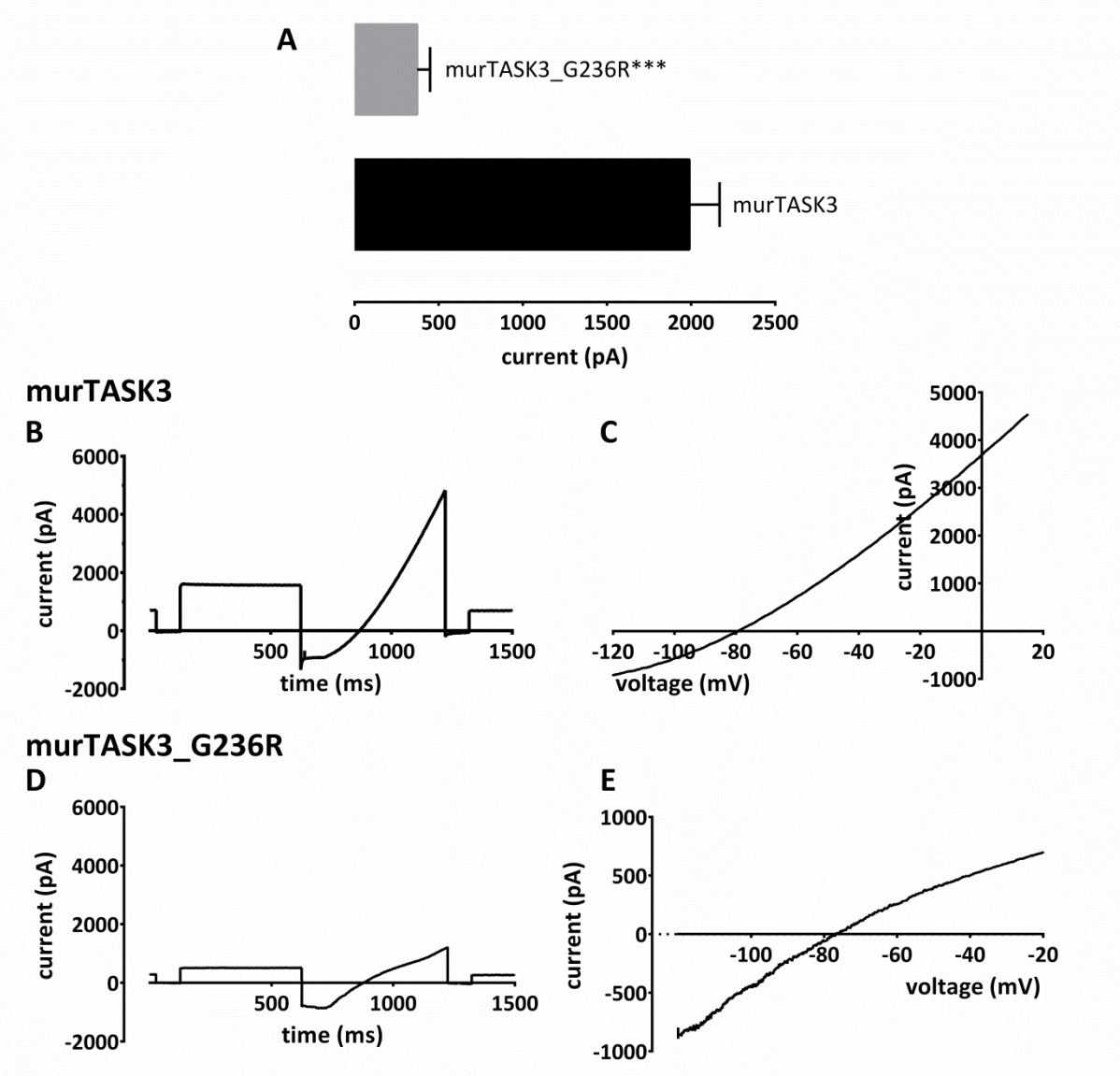

Supplementary Figure 3